

208
MAY 5 1972

RECEIVED BY TIC MAY 18 1972

Research Report

SC-RR-71 0673

May 1972

MASTER

APPLICATION OF HEXANITROSTILBENE (HNS)
IN EXPLOSIVE COMPONENTS

Alfred C. Schwarz
Explosive Components Division, 1914
Sandia Laboratories, Albuquerque

DISTRIBUTION OF THIS DOCUMENT IS UNLIMITED

SANDIA LABORATORIES



OPERATED FOR THE UNITED STATES ATOMIC ENERGY COMMISSION BY SANDIA CORPORATION | ALBUQUERQUE NEW MEXICO LIVERMORE CALIFORNIA

Issued by Sandia Corporation,
a prime contractor to the United States Atomic Energy Commission

NOTICE

This report was prepared as an account of work sponsored by the United States Government. Neither the United States nor the United States Atomic Energy Commission, nor any of their employees, nor any of their contractors, subcontractors, or their employees, makes any warranty, express or implied, or assumes any legal liability or responsibility for the accuracy, completeness or usefulness of any information, apparatus, product or process disclosed, or represents that its use would not infringe privately owned rights.

DISCLAIMER

This report was prepared as an account of work sponsored by an agency of the United States Government. Neither the United States Government nor any agency Thereof, nor any of their employees, makes any warranty, express or implied, or assumes any legal liability or responsibility for the accuracy, completeness, or usefulness of any information, apparatus, product, or process disclosed, or represents that its use would not infringe privately owned rights. Reference herein to any specific commercial product, process, or service by trade name, trademark, manufacturer, or otherwise does not necessarily constitute or imply its endorsement, recommendation, or favoring by the United States Government or any agency thereof. The views and opinions of authors expressed herein do not necessarily state or reflect those of the United States Government or any agency thereof.

DISCLAIMER

Portions of this document may be illegible in electronic image products. Images are produced from the best available original document.

SC-RR-71 0673

APPLICATION OF HEXANITROSTILBENE (HNS) IN EXPLOSIVE COMPONENTS

Alfred C. Schwarz
Explosive Components Division, 1914
Sandia Laboratories, Albuquerque, N. M. 87115

Printed May 1972

ABSTRACT

This report provides design information on the utilization of hexanitrostilbene (HNS) in explosive components.

Performance data are presented for aluminum-sheathed, linear shaped charge (ALSC). An introduction to such components as shielded detonating train (SDT) and mild detonating fuze (MDF) employing HNS is also made.

Key Words: hexanitrostilbene, design information, ALSC, explosive components.

NOTICE

This report was prepared as an account of work sponsored by the United States Government. Neither the United States nor the United States Atomic Energy Commission, nor any of their employees, nor any of their contractors, subcontractors, or their employees, makes any warranty, express or implied, or assumes any legal liability or responsibility for the accuracy, completeness or usefulness of any information, apparatus, product or process disclosed, or represents that its use would not infringe privately owned rights.

DISTRIBUTION OF THIS DOCUMENT IS UNLIMITED

ACKNOWLEDGMENT

Several associates contributed significantly toward providing the information contained herein. Paul E. Matson, Division 1914, performed many of the tests and prepared many of the specimens required for the experiments. Robert J. Buxton and T. M. Massis, Division 1915, provided much of the data relating to the physical properties, as well as most of the photomicrographs.

TABLE OF CONTENTS

<u>SECTION</u>	<u>Page</u>
I INTRODUCTION	6
II GENERAL PROPERTIES	7
III POWDER HANDLING PROPERTIES	9
Compaction Properties	9
Photomicrographs	10
IV DETONATION PROPERTIES	12
Detonation Velocity vs Density	12
Shock Initiation Sensitivity	14
Impact Sensitivity	17
Hydrocompaction	17
Minimum-Use Diameter	18
V COMPATIBILITY OF HNS WITH OTHER MATERIALS	20
VI HAZARD INFORMATION	21
Health Hazards	21
Stray Energy Hazard	21
VII ALUMINUM-SHEATHED LINEAR SHAPED CHARGE	22
Principles of Function	22
Rupturing Ability	24
Impulse Generated During Detonation	28
Application Principles	29
VIII ENVIRONMENTAL CAPABILITIES	30
Thermal Stability	30
Detonation Velocity	30
Rupturing Ability	31
Discoloration	31
Shock Initiation	33
Weight Loss	34
Effect of Heating Rates	34
Function at High Temperature	36
Radiation	36
Effect of Moisture	37
High Altitude (low pressure)	38
IX TYPICAL APPLICATIONS OF HNS	39
Aluminum-Sheathed Linear Shaped Charge	39
Shielded Detonating Train	40
Mild Detonating Fuze	41
End Fittings	42
X REFERENCES	43

LIST OF ILLUSTRATIONS

<u>Figure</u>		<u>Page</u>
I-1	Structural Formula for HNS	6
II-1	DTA Summary	8
III-1	Compaction Pressure vs Density of Explosive Materials	9
III-2	Photomicrographs of Explosive Materials	11
IV-1	Detonation Velocity vs Density of HNS-II	12
IV-2	Detonation Velocity vs Powder Density	13
IV-3	Barrier Thickness for 50 Percent Probability of Initiation of Five Explosives	15
IV-4	Threshold Initiation Pressure of Several Explosives as a Function of Diameter and Density	16
IV-5	Probability of Explosion from Drop Hammer Impact	17
IV-6	Effect of Hydrostatic Compaction on Performance of ALSC	18
IV-7	Detonation Velocity vs Core Diameter ⁻¹ for Aluminum-Sheathed, HNS-Core MDF	19
VII-1	Aluminum-Sheathed Linear Shaped Charge	22
VII-2	Evolution of ALSC Shapes	23
VII-3	Cross-Section Dimensions for ALSC	23
VII-4	Optimum Standoff Distance	24
VII-5	Optimum Liner Angle	25
VII-6	Suggested Setup for Rupturing Ability and V_D Testing	26
VII-7	Effect of Core Load on Rupturing Ability of Aluminum 6061 and Mild Steel	27
VII-8	Effect of Loading Distribution on Impulse	28
VIII-1	Effect of Thermal Aging on Decrease in V_D of Explosive Materials	30
VIII-2	Reduction in Rupturing Ability as a Function of Reduction in V_D Produced by Thermal Aging	31
VIII-3	Discoloration of HNS as a Result of Thermal Aging	32
VIII-4	Effect of Thermal Aging on Detonation Velocity and Barrier Thickness for 50 Percent Probability of Initiation of HNS	33
VIII-5	Weight Loss vs Time at 500°F	34
VIII-6	Heat Absorbed on Surface of ALSC vs Time to Reaction	35
VIII-7	Effect of Heating Rate on Reaction Temperature	35
VIII-8	Reactor Radiation Required to Produce a 1 Percent Weight Loss	37
IX-1	ALSC in Teflon Holding Strip	39
IX-2	Cross Section, SDT Tip	40
IX-3	SDT Distribution Train	40
IX-4	MDF	41
IX-5	End Fittings	42

LIST OF TABLES

<u>Table</u>		<u>Page</u>
II-I	Certain Properties of Interest	7
IV-I	Threshold Initiation Pressure for HNS-II	14
IV-II	Summary of Data, Test Specimens for Minimum-Use-Diameter Study	19
V-I	Summary of Compatibility Data	20
VI-I	Summary of Health Hazard Test Data	21
VIII-I	Effect of Temperature on Detonation Velocity (10-grain/foot ALSC (HNS))	36
VIII-II	Summary of High-Altitude Tests (10-grain/foot ALSC (HNS))	38

SECTION I - INTRODUCTION

This document provides design information for the utilization of one of the new, thermally stable explosives in linear shaped charges and other devices which may be subjected to temperatures as high as 500°F.

Pertinent data relative to some available explosives were reviewed. Hexanitrostilbene (HNS) was selected for further study on the basis of these data and with due consideration for its notable success in end boosters on the Apollo program¹ and in Department of Defense applications.² A comparison of some of the HNS properties relative to more common explosives is contained in this report.

A simple one-step process, using TNT as a starting material, makes HNS one of the most easily prepared of the series of thermally stable explosives.³ The very fine crystalline material obtained from the reaction, purified only by extraction of impurities, is designated as HNS-I. HNS-II is a larger particle-size, higher bulk-density, free-flowing material obtained by recrystallization of HNS-I. At present, only one crystalline form of HNS, from room temperature up to its melting point, is believed to exist.

All aluminum-sheathed linear shaped charge (ALSC) and mild detonating fuze (MDF) applications employ the Type II version; the only known application for Type I material is in end boosters in shielded detonating trains (SDT's), where a quality level of 0.9995 at 90 percent confidence has been demonstrated.²

Unless otherwise stated, data reported herein are based on the HNS identified as Type II, the structural formula of which is shown in Figure I-1. An "A" designation after the type number indicates that acceptance testing included initiation sensitivity, whereas "B" indicates acceptance to the specification but that the sensitivity tests were not performed. HNS may be procured against Navy specification WS-5003.

2, 2', 4, 4', 6, 6'

Hexanitrostilbene

HNS

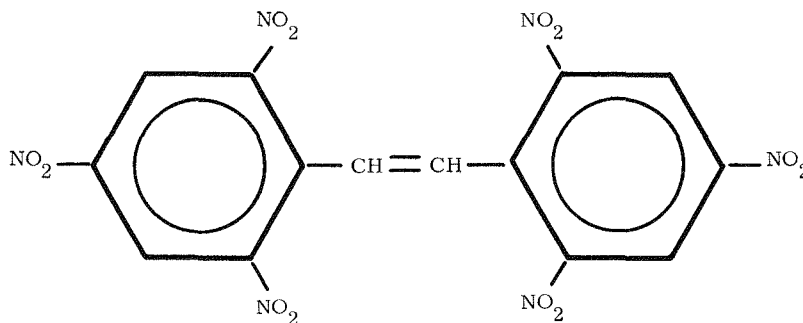


Figure I-1. Structural Formula for HNS

Aluminum-sheathed, linear shaped charge and aluminum-sheathed MDF (round or ribbon-shaped) which contain HNS core explosive have been developed at the Sandia Laboratories. Development was required to satisfy a classified system application.

SECTION II - GENERAL PROPERTIES

This section deals with some of the properties of general interest. Comparative data on contemporary explosives are shown in Table II-I.

TABLE II-I
Certain Properties of Interest

	HNS-II	HMX	HNAB	PETN
Lot Identification	43-13	63-204-2-2	43-11	741
Color	yellow-buff	white	orange	white
Max Theoretical Density (grams/cm ³)	1.74	1.90	1.76	1.77
Bulk Density (grams/cm ³)	0.36	0.66	0.64	0.29
Melting Point (°C)	318	285	220	140
Specific Heat (cal/gram/°C)	--	0.28	--	--
Vapor Pressure at 100°C (mm Hg)	1x10 ⁻⁹	3x10 ⁻⁹	1x10 ⁻⁷	8x10 ⁻⁵
Linear Coefficient of Thermal Expansion (cm/cm/°C)	9.2x10 ⁻⁵	5.0x10 ⁻⁵	8.0x10 ⁻⁵	11.3x10 ⁻⁵
Resistivity ¹⁴ (ohm-cm)	5x10 ¹³	4x10 ¹⁰	--	3x10 ¹²
Dielectric Strength (volts/mil)	400	90	--	130
Heat of Explosion				
(cal/gram)	958	1360	1030	1380
(kJ/gram)	4.0	5.7	4.3	5.8
Volume of Detonation Gases at STP (cm ³ /gram)	756*	908	780	780

Note: While these data are believed to be representative of the explosives, they are from a wide variety of sources. If a property has a significant effect on end application, it is suggested that the test be rerun.

* Measured in a large chamber after temperature stabilization. One gram of HNS produced a gas pressure increase of 7.55 psi/100 in.³ of volume. If the gas temperature reaches the theoretical detonation temperature prior to stabilization, the pressure may reach 20 times this value.

The DTA data of Figure II-1 indicate a similarity among PETN, HNAB, and HNS in that these three exhibit little decomposition (exotherm) prior to melting (endotherm). HNAB is exceptional in that there is a large temperature difference between the melting point (225°C) and rapid decomposition (at 350°C); the perturbation at 190°C indicates solvent evolution and/or a minor crystal phase change. HMX shows the beta-delta phase transition at 190°C and a rapid decomposition immediately prior to its melting temperature (285°C).

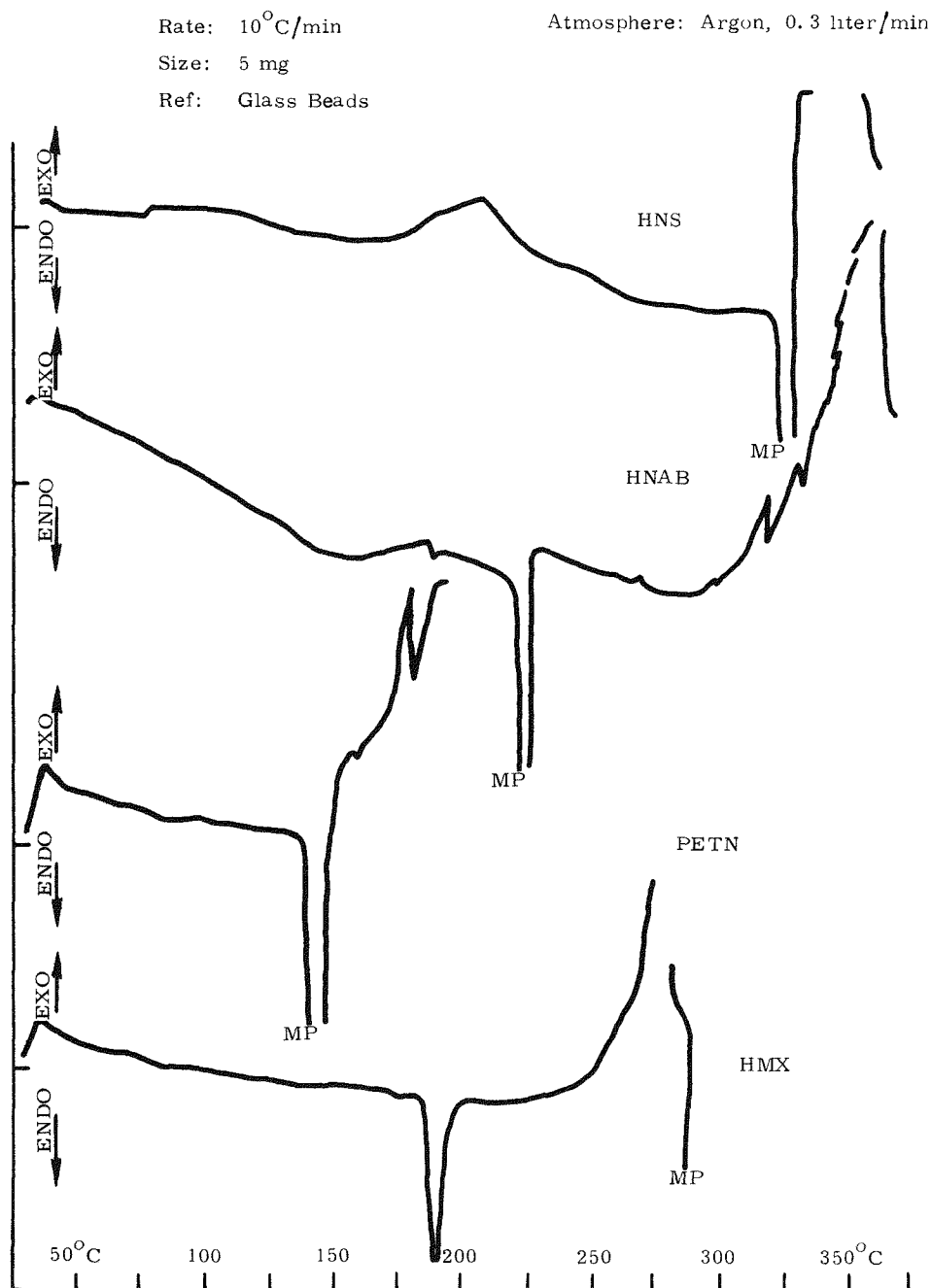


Figure II-1. DTA Summary

SECTION III - POWDER HANDLING PROPERTIES

Compaction Properties

In explosive device applications, it is necessary to refer to compaction data in order to design loading tools and to provide structurally sound hardware. Many factors enter into the exact relationship between average powder density in a container and the ram force required to provide that compaction. Factors which affect this relationship, although not demonstrated herein, include ram clearance, moisture content of powder (even though less than 0.1 percent), strength of container, powder particle size, and surface finish in container.

Typical pressure-density relationships are shown in Figure III-1. A ram diameter of 1/8 inch, a powder column length of 1/8 inch, and thick-walled metallic containers were employed to obtain these data. The ram/wall clearance was 0.004 inch on the diameter.

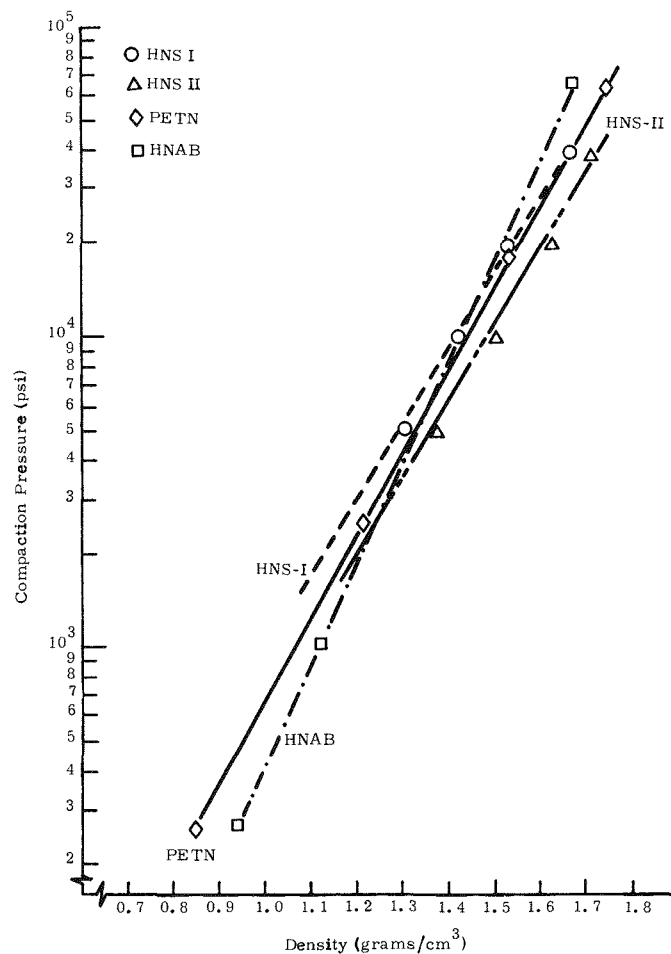


Figure III-1. Compaction Pressure vs. Density of Explosive Materials

Some points of interest are as follows:

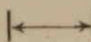
- (1) There is a linear relationship between the loading density and the logarithm of the loading pressure.
- (2) HNS-I requires a higher compaction pressure than HNS-II to produce a given density. A possible explanation is that, inasmuch as HNS-I has a lower bulk density, wedging of particles has more opportunity to occur and physical crushing of the finer particles requires more pressure.
- (3) If loading pressure alone is used as a control of density during fabrication of a device, the density-pressure relationship should be established in the "as-used" hardware.
- (4) The slope of the compaction pressure vs density line is a measure of the expected reproducibility of the device into which the explosive is placed. Both detonation velocity and shock pressure are related to explosive density.

Photomicrographs

As stated in Section I, Type II HNS consists of larger particles with a higher bulk density than Type I HNS; Type II is thus a more free-flowing powder and is more amenable to manufacture into aluminum-sheathed linear shaped charge or mild detonating fuze.

The particles are shown in the photomicrographs of Figure III-2. For comparison purposes, typical photomicrographs of HNAB, PETN, and HMX are also shown.



100
Microns 

HNS-1
Lot 43-39
 $S_o^p = 12,500 \frac{\text{cm}^2}{\text{gm}}$



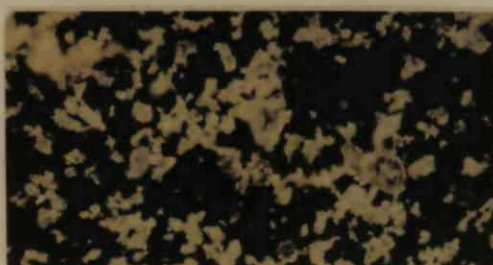
HNS-II
Lot 43-13
 $S_o^p = 4850 \frac{\text{cm}^2}{\text{gm}}$



PETN Type 1
Batch 741
 $S_o^p = 3880 \frac{\text{cm}^2}{\text{gm}}$



HNAB
Lot 43-11
 $S_o^p = 940 \frac{\text{cm}^2}{\text{gm}}$



HMX
Lot 63-202-2-2
 $S_o^p = 2950 \frac{\text{cm}^2}{\text{gm}}$

Figure III-2. Photomicrographs of Explosive Materials (at 125X). Specific Surface Area, S_o^p , Was Determined by Air Permeability Technique.

SECTION IV - DETONATION PROPERTIES

Detonation Velocity vs Density

The density at which the explosive is loaded into a device affects detonation velocity, shock pressure generated, initiation sensitivity, distance to detonation, and jet characteristics, as well as other characteristics.

Measurements were made⁴ to determine the detonation velocity of HNS-II as a function of its density for two column diameters. Data are shown in Figure IV-1. It should be noted that there was a diameter effect on velocity. The "infinite diameter" detonation velocity was calculated on the basis that detonation velocity is a linear function of the reciprocal of the charge diameter.

A similar determination for HNS-I indicated its velocity to be independent of diameter for the diameters tested and to replicate the "infinite diameter" velocity for HNS-II.

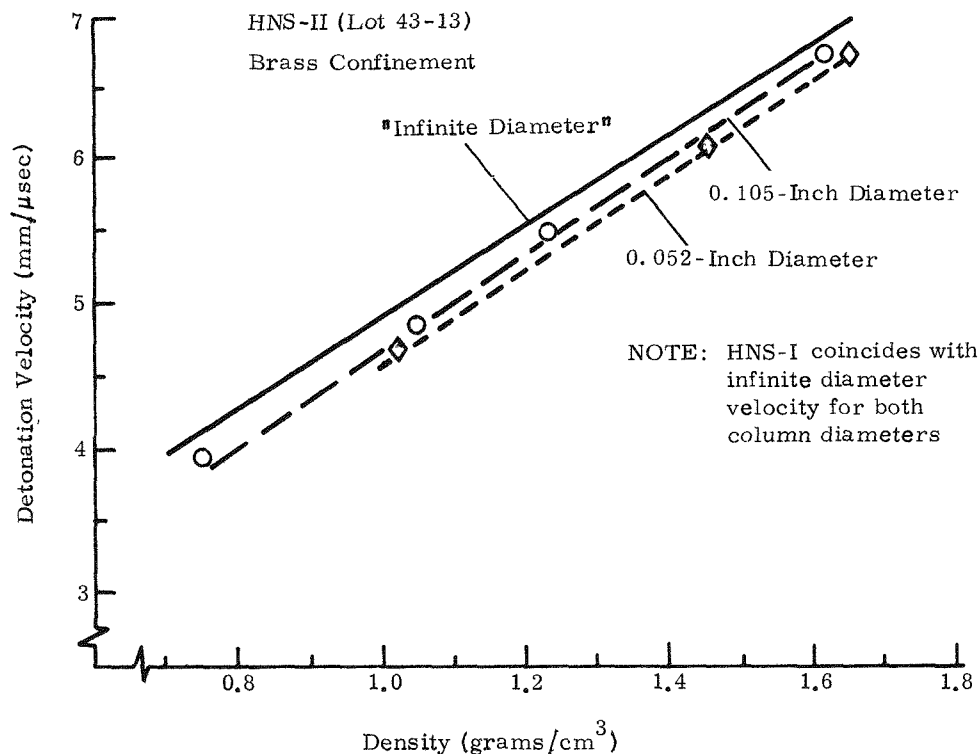


Figure IV-1. Detonation Velocity vs Density of HNS-II

The detonation velocity data are shown in Figure IV-2 for heavily confined columns 1/8 inch in diameter for HNS-Type II, HNAB, and PETN. The slope of the line for each explosive is another indication of its reproducibility in an application. Values, as shown, range from 3150 to 3900

$$\frac{\text{m/sec}}{\text{grams/cm}^3}$$

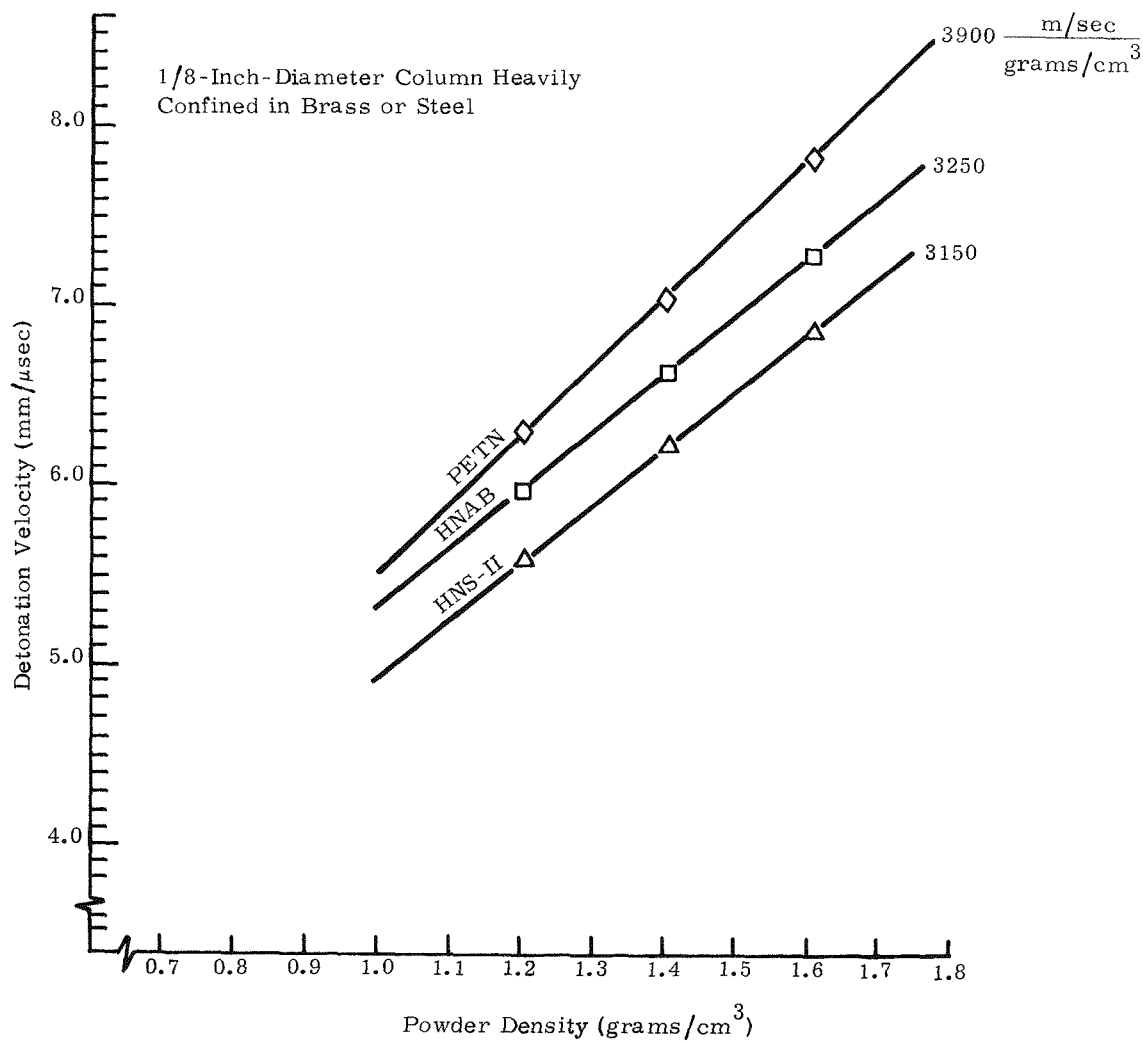


Figure IV-2. Detonation Velocity vs Powder Density

Shock Initiation Sensitivity

It is often necessary to know the shock pressure required to initiate HNS-II on a 50 percent probability (or threshold) basis. Density and donor size are two of the parameters which affect sensitivity. Data on relatively large diameter charges of HNS-II are presented in Table IV-I.

TABLE IV-I
Threshold Initiation Pressure* for HNS-II

	<u>Density, Percent of Theoretical Maximum</u>	
	<u>80%</u>	<u>90%</u>
<u>Initiation Pressure at 77°F (kilobars)</u>		
1/2-Inch Donor	17	23
8-Inch Plane Wave Lens	12	18 [†]
 <u>Initiation Pressure at 500°F (kilobars)</u>		
8-Inch Plane Wave Lens	-	11

* Threshold initiation pressure which will produce initiation on a 50 percent probability basis. This work was performed on Sandia Contract 58-1348 by Stanford Research Institute and was completed in August 1967.

[†] Value for PETN under identical conditions was 9.

As a guide for hardware design, the data of Figure IV-3 provide relative initiation sensitivities of five explosives. In this test, an aluminum barrier is placed between the test explosive and a standard detonating charge (in this case a commercial subminiature, exploding bridgewire detonator containing about 65 milligrams of PETN). The barrier thickness is varied to establish that value which will produce a 50 percent probability of detonation of the test explosive. In this figure, greater barrier thicknesses indicate easier initiation.

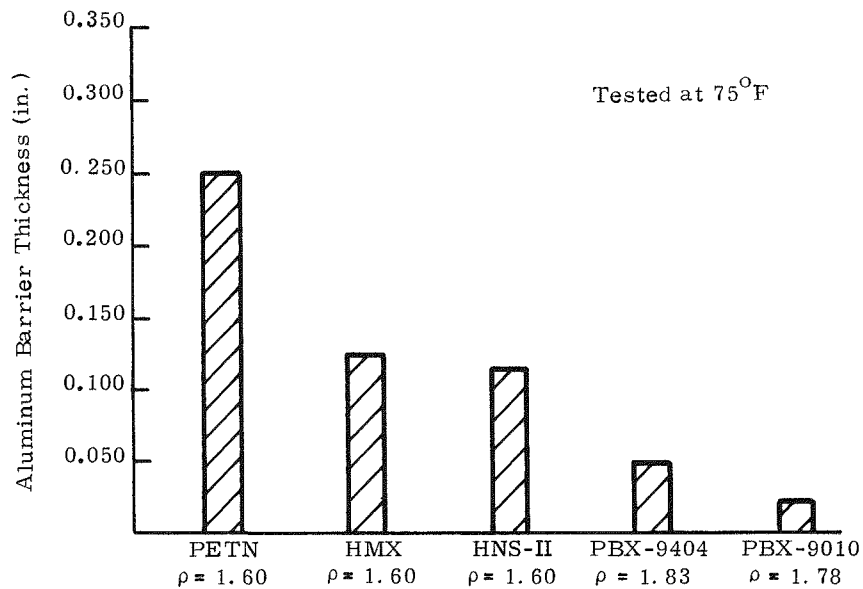
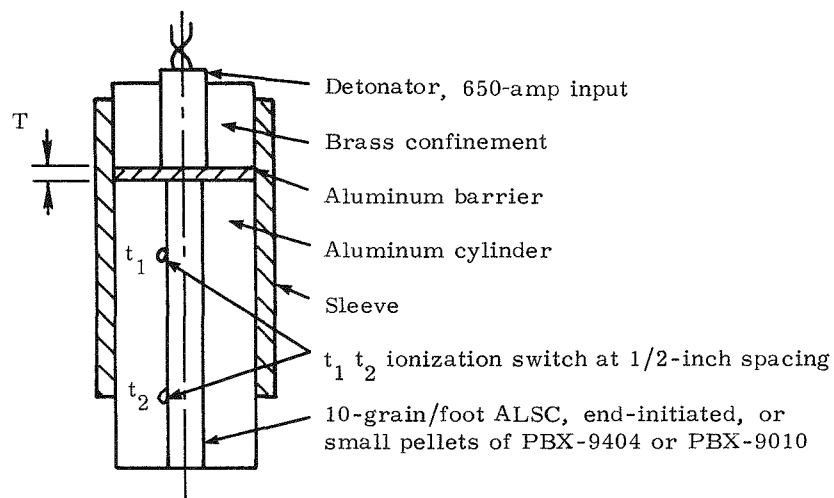


Figure IV-3. Barrier Thickness for 50 Percent Probability of Initiation of Five Explosives

The effect of powder density on initiation sensitivity in very small diameters is shown in Figure IV-4. The ordinate is an arbitrary scale "scaled decibang," which is related to shock pressure; this scale is described more fully in Reference 4, from which the data were extracted. The data show the relative importance of density and column diameter on the initiation sensitivity* of four different explosives. In this figure, higher values of SDB_g indicate greater difficulty to initiate. An approximate value of equivalent threshold initiation pressure was established in Reference 17 and is also shown in Figure IV-4.

HNS is one of six boosting explosives permitted by the DOD to be in line with the main charge, without an interrupter, in high-explosive warheads. Details are contained in MIL-STD-1316A, "Design Safety Criteria for Fuzes."

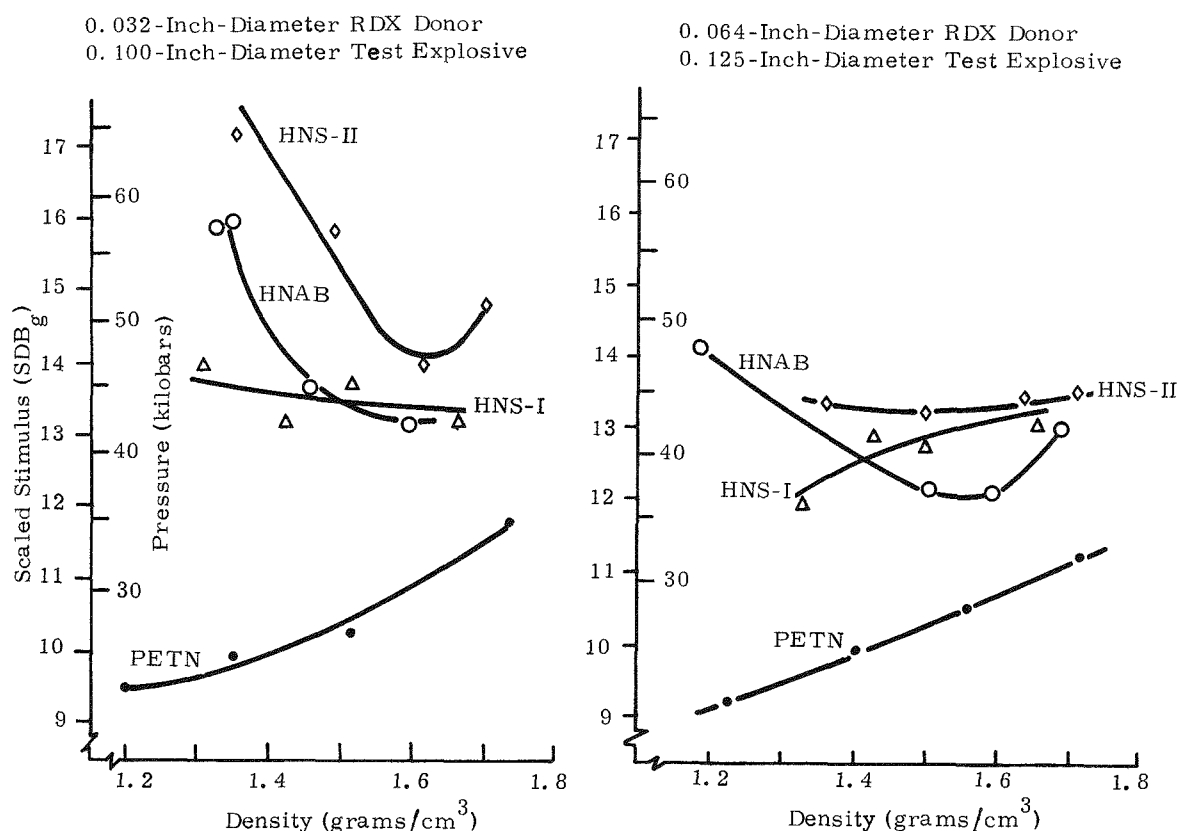


Figure IV -4. Threshold Initiation Pressure of Several Explosives as a Function of Diameter and Density

* Shock duration also plays an important role in initiation sensitivity; data are not currently available for HNS.

Impact Sensitivity

Drop hammer tests provide supplementary data on initiation sensitivity. This information is useful to those concerned with pressing explosives, with other facets of hardware assembly, or with in-plant transportation of explosive components. The data are summarized in Figure IV-5, along with data for other explosives. It is noteworthy that HNS showed a broad range of drop heights which produced an "explosion"; at the smaller drop height, the "explosion" consumed less of the test specimen than for the larger drop height. In the case of PETN, it was more nearly a go/no-go "explosion."

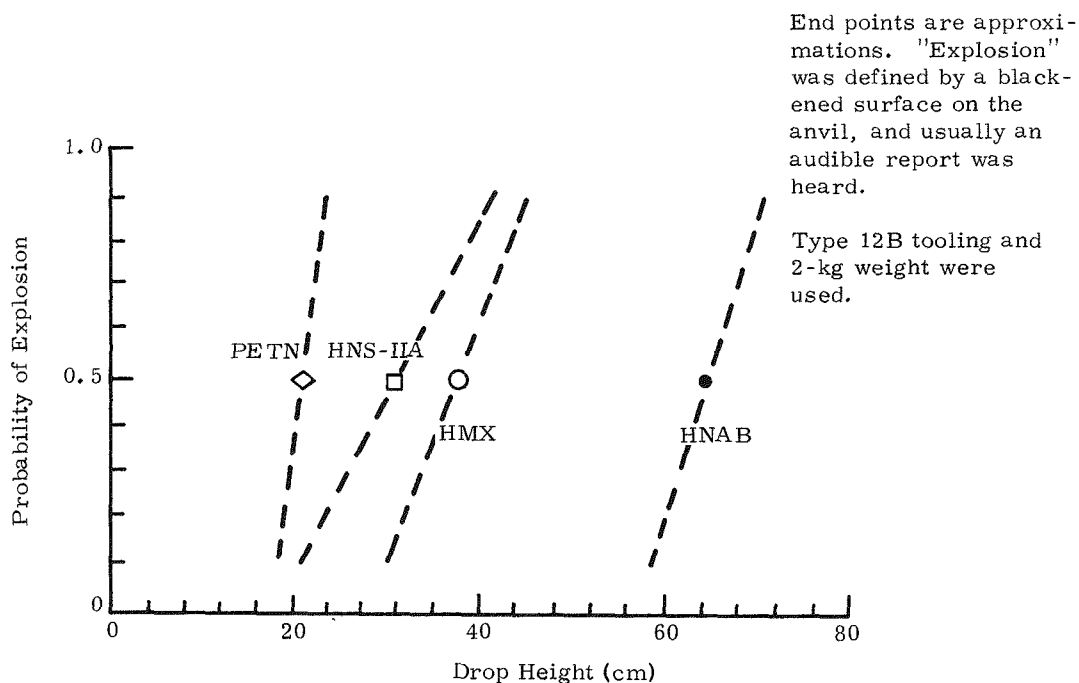


Figure IV-5. Probability of Explosion From Drop Hammer Impact

Hydrocompaction

A technique developed at Sandia to reduce the unit-to-unit variation in the detonation time of mild detonating fuze was extended to applications employing HNS.

Hydrocompaction of 30,000, 50,000, and 70,000 psi was applied to HNS-core ALSC to determine its effect on detonation velocity, core density,⁵ and rupturing ability.

Data are summarized in Figure IV-6. Hydrocompaction at 65,000±5000 psi increased the rupturing ability of ALSC.

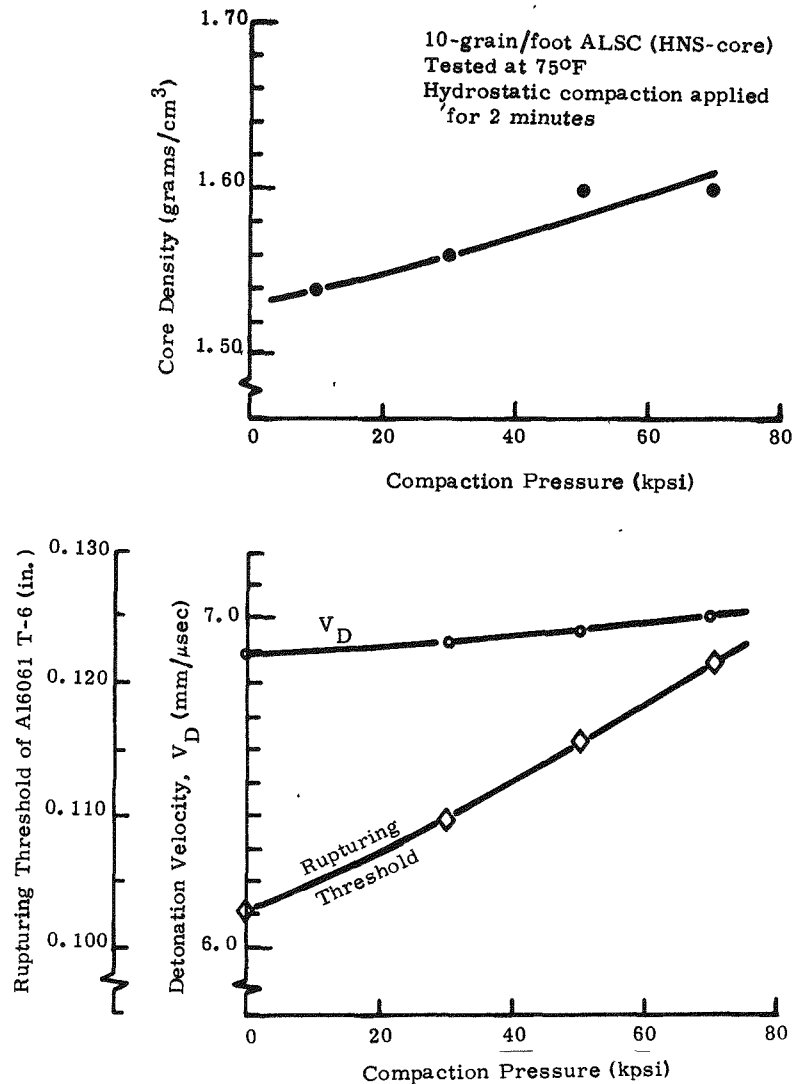


Figure IV-6. Effect of Hydrostatic Compaction on Performance of ALSC

Minimum-Use Diameter

Component miniaturization requires knowledge of the minimum (or critical) diameter in which full detonation velocities may be achieved and sustained. Accordingly, mild detonating fuze containing HNS was fabricated in aluminum sheathing and evaluated.

Pertinent pretest dimensions are contained in Table IV-II. Detonation velocity was determined as a function of core loading. The results (Figure IV-7) indicated that the minimum recommended-use diameter* for the uncompacted MDF was 1 grain/foot and that this was 1/2

* The explosive column diameter is often indicated by referring to the core loading in grains/foot length (assuming that explosive density is constant). There are 15.43 grains/gram.

grain/foot for the hydrocompacted material. There is no implication intended that minimum-use diameter is a linear function of density or that all explosives behave similarly. Chapter 1.5 in Reference 16 contains useful information on this subject.

TABLE IV-II
Summary of Data
Test Specimens for Minimum-Use-Diameter Study

Nominal Core Loading (grains/foot)	As-Fabricated		After Hydrocompaction		
	OD (in.)	OD (in.)	ID (in.)	Wall Thickness (in.)	Core Density (gm/cm ³)
10	0.1110	0.1100	0.0520	0.029	1.66
5	0.0800	0.0795	0.0360	0.022	1.66
2-1/2	0.0590	0.0586	0.0265	0.016	1.67
1	0.0325	0.0324	0.0135	0.010	1.66
1/2	0.0238	0.0237	0.0108	0.007	1.65
1/4	0.0180	0.0180	0.0073	0.005	1.65

Note: All lots were tamp-filled and 100 percent swaged to final outside diameters.

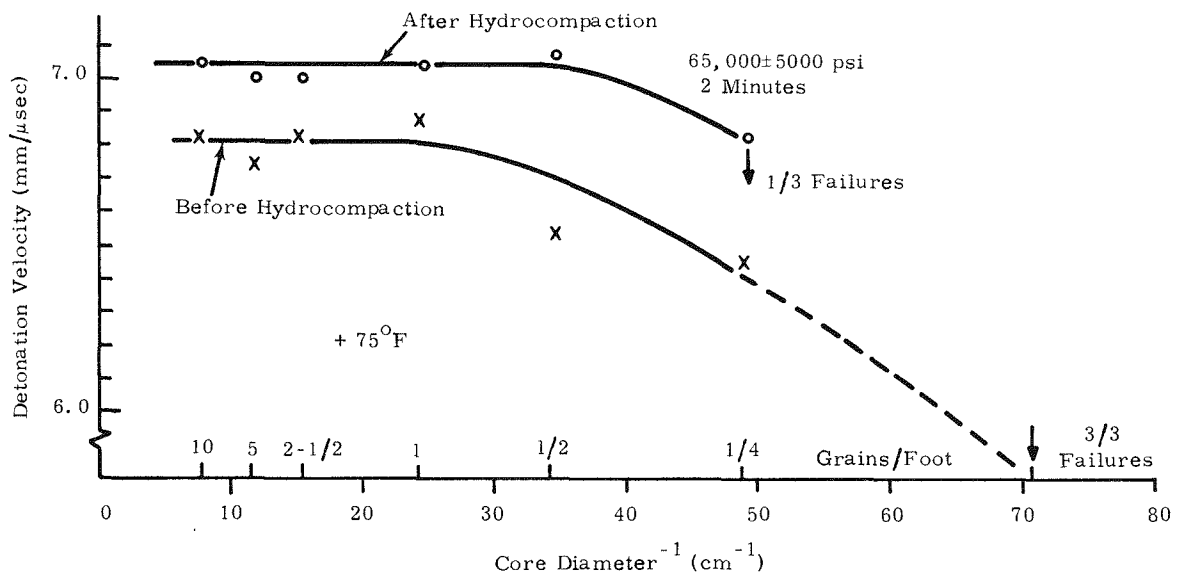


Figure IV-7. Detonation Velocity vs Core Diameter⁻¹ for Aluminum-Sheathed, HNS-Core MDF

SECTION V - COMPATIBILITY OF HNS WITH OTHER MATERIALS

One engineering requirement for component design is that the specific explosive and the adjacent material, be it structural or otherwise, may be in close proximity to each other without deterioration of either.

The compatibility tests, devised and performed on many combinations, are fully described in Reference 6. The Type I test is basically a vacuum stability test in which the quantity of off-gas from the combination is compared to that from a standard; if the test specimen produces more than five times the off-gas than that from the standard, the combination is declared incompatible. Type 2 tests employ microscopy, color changes, or metallurgical changes to establish incompatibility.

TABLE V-I
Summary of Compatibility Data

<u>Compatible Combinations</u>			
<u>Material</u>	<u>Test Type</u>	<u>Test Temp (°F)</u>	<u>Time (hr)</u>
<u>Explosives</u>			
1. HNS + PETN	2	165	168
2. HNS + HMX	1	250	96
3. HNS + PBX-9407	1	250	96
<u>Structural</u>			
1. HNS + Teflon	1	250	96
	2	500	168
2. HNS + Aluminum	2	500	168
3. HNS + Stainless Steel (Type 303)	2	500	168
<u>Adhesives and Encapsulants</u>			
1. HNS + Eastman 910	2	75	--
2. HNS + Fastbond 2210 (uncured)	2	165	168
	1	250	96
3. HNS + Epoxylite 8822 (uncured)	1	250	96
4. HNS + Adiprene L-100 MOCA, Polyol (uncured)	2	75	--
5. HNS + Epon 810 (3-part system) (uncured)	2	210	24
6. HNS + PSR 501 (Polysulfide, cured and uncured)	1	250	48
<u>Miscellaneous</u>			
1. HNS + Hydrocompaction Oil A*	2	75	120
Oil B**	2	160	290
<u>Incompatible Combinations</u>			
<u>Material</u>	<u>Test Type</u>	<u>Test Temp (°F)</u>	<u>Time (min)</u>
1. HNS + Armstrong C-7 With Activator W (uncured)	2	75	1
2. HNS + Epon 828-Versamid 140	2	75	--

* K-10 hydraulic fluid from ORE-LUBE, College Point, New York

** Chevron NF-5 mineral oil

SECTION VI - HAZARD INFORMATION

Health Hazards

An investigation⁷ was performed on the irritancy and toxicity of HNS. A summary of the toxicologist's report follows:

HNS was nontoxic and nonirritating when in contact with the skin. The mild and transitory eye irritancy was reduced by rapid and thorough washing with water. The low acute oral toxicity suggests that no significant adverse effects are likely to be encountered in routine industrial handling.

Table VI-I is a brief tabulation of results from each of the four tests performed, as well as comparative results on HNAB.

TABLE VI-I
Summary of Health Hazard Test Data

	HNAB	HNS
Primary Skin Irritancy Index	0*	0*
Primary Eye Irritancy	Mild & Transitory 2.7 @ 24 hr†	Mild & Transitory 1.3 @ 24 hr†
Single-Dose Percutaneous††Toxicity	> 2000 mg/kg	> 2000 mg/kg
Single-Oral** -Dose Toxicity (LD ₅₀)	3482 mg/kg	> 4000 mg/kg

* Nonirritating; tests performed on rabbits.

† Unwashed; 20 is greatest irritancy; tests performed on rabbits.

†† Samples applied to 10 percent of body area of unabraded backs of rabbits.

** Given intragastrically to young male rats.

Stray Energy Hazard

As part of a study of the effects of stray energy hazards on ALSC, a series of drop tests was performed to determine whether initiation of the HE could result from this input. A 26-pound hemispherical-nosed weight was dropped from heights up to 40 feet on well-supported test specimens.

Test Sample	ALSC Held Between Two 4x4x1/2-Inch Aluminum Plates		Max Drop Height (ft)	Observed Reaction
	Constrained	Not Constrained		
10-Grain/Foot ALSC(HNS)	X	X	40	None
10-Grain/Foot ALSC(HMX)	X		40	None

SECTION VII - ALUMINUM-SHEATHED LINEAR SHAPED CHARGE

Principles of Function

ALSC is a continuous explosive core enclosed in a seamless aluminum sheath. Shaped in the form of a chevron, the continuous liner and explosive produce a linear rupturing action. This application is enhanced by careful control of charge dimensions and configuration.

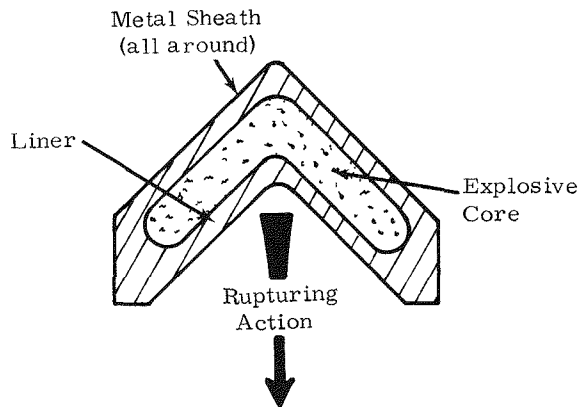


Figure VII-1 Aluminum-Sheathed Linear Shaped Charge

The explosive phenomenon is generally described as the interaction of the detonation products and cavity liner material. The explosive reaction releases large quantities of gas; shock waves, followed by the expanding gases, move outward radially as well as longitudinally and conform generally in shape to the ALSC cross section. The shock waves emanating from the lower portion of the ALSC converge in a plane parallel to the ALSC axis and cause an extreme pressure concentration along the plane of convergence. These directed shock waves, together with the gaseous products of detonation and the metal from the sheathing material, produce the rupturing action. Deformation of the target material begins within microseconds of the passage of the detonation front at any given point on the ALSC; complete rupturing of the target occurs within a tens of microseconds.

Typically, if a length of ALSC is detonated on a metal witness plate, the jet exerts a force along a very narrow line. This force causes the metal to be pushed out of the way of the advancing jet by plastic flow. The resulting groove is commonly termed "penetration." On a thin plate, however, the performance of ALSC depends not only on the cavity liner material and the intense directed shock waves to erode the target but also on the rapidly expanding gases to physically dislocate and fracture it. The shock waves, when reflected from the surface opposite the cut, can also cause spalling from that surface. The total effect is termed "rupturing." ALSC consistently ruptures a target metal nearly twice the thickness of the jet penetration.

Early in the development of mild detonating fuze, it became evident that a directional effect could be realized by shaping. The evolution of shapes is shown in Figure VII-2. A configuration similar to those shown as Types III and IV has been standardized. These shapes may be twice as effective for rupturing purposes as MDF's of equivalent core load. Dimensions are shown in Figure VII-3.

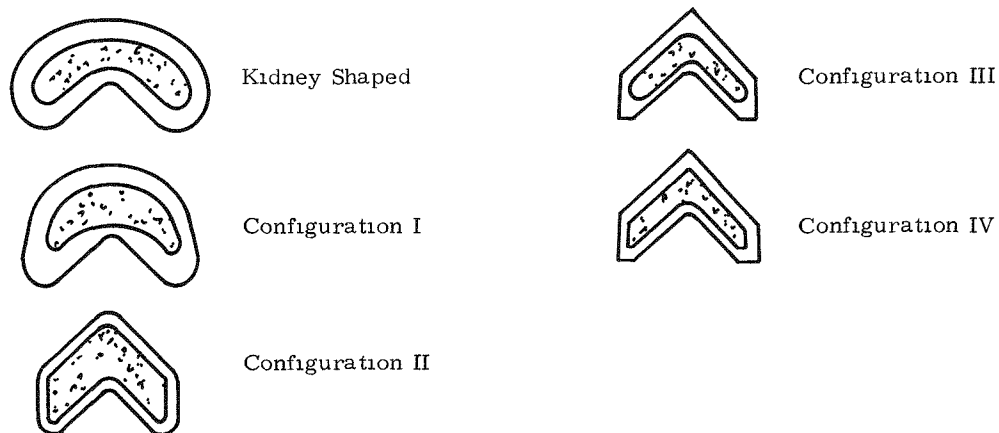
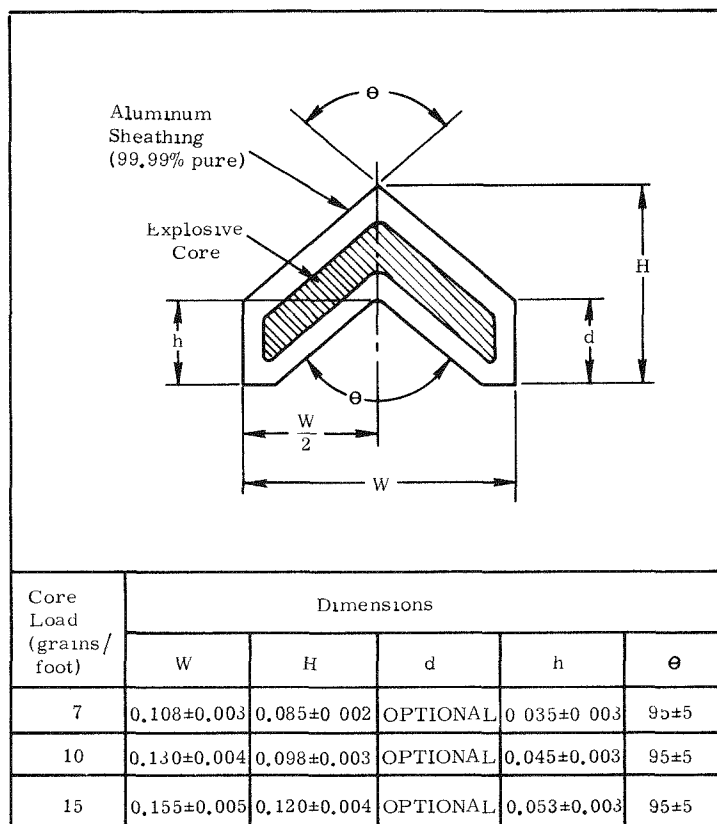


Figure VII-2. Evolution of ALSC Shapes



NOTE. All dimensions are in inches except θ , which is in degrees.

Figure VII-3. Cross-Section Dimensions for ALSC

Rupturing Ability

Aluminum sheathing of high purity was selected for its favorable temperature and its strength and weight properties. In addition, it has experienced a successful production history in high-quality, mild detonating fuze (MDF) for Sandia applications. An aluminum panel, a common material in flight test vehicles, was chosen as a typical structural material to be ruptured.

Extruded teflon, chosen to hold the ALSC in place, is designed to provide the optimum standoff distance from the panel to be ruptured. It has a high temperature capability, is relatively inexpensive, provides some shock mitigation to surrounding structure, and may be readily fastened in place.

The optimum position of the ALSC with respect to a panel to be ruptured may be determined by experiment. Optimum standoff for HNS is shown in Figure VII-4, along with comparative data for HMX. Optimum standoff for 10-grain/foot ALSC (HNS) on aluminum panels was in the range of 0.034 to 0.050 inch. (The same range was observed for 7- and 15-grain/foot samples.)

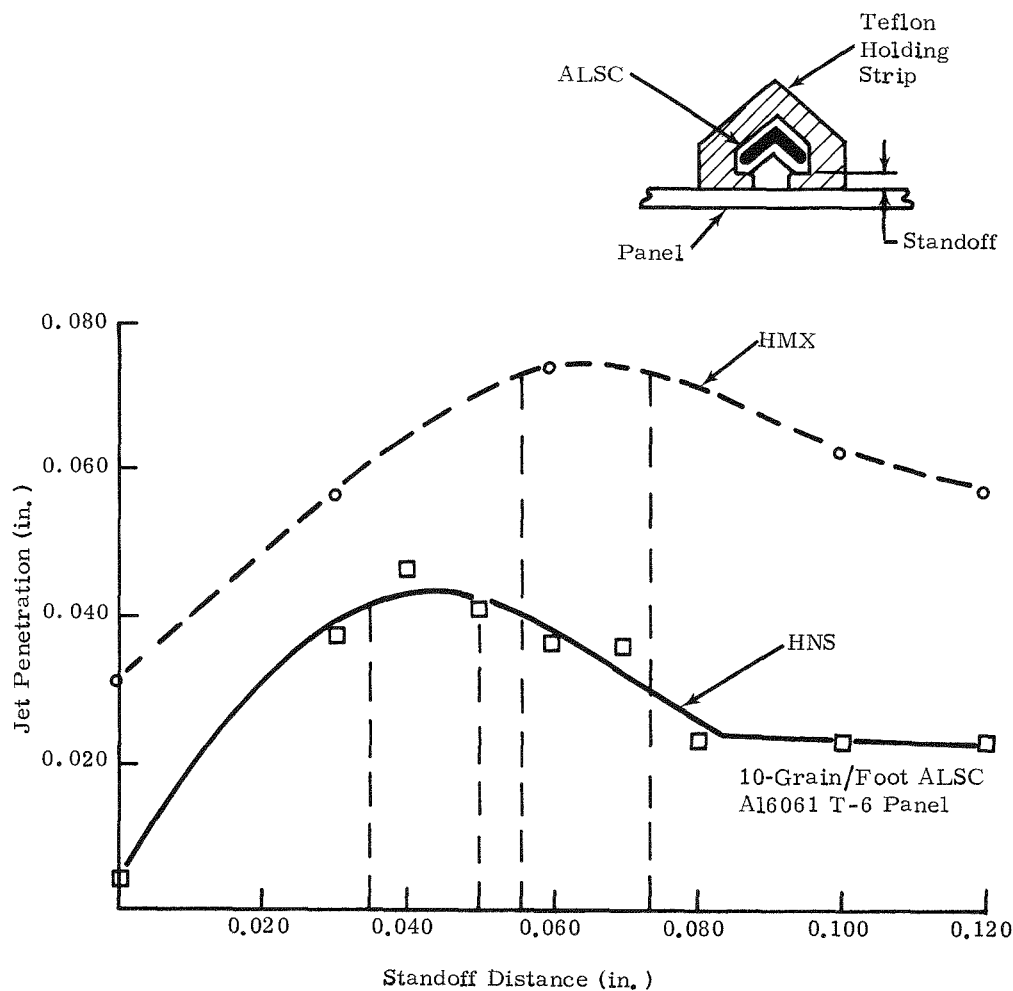
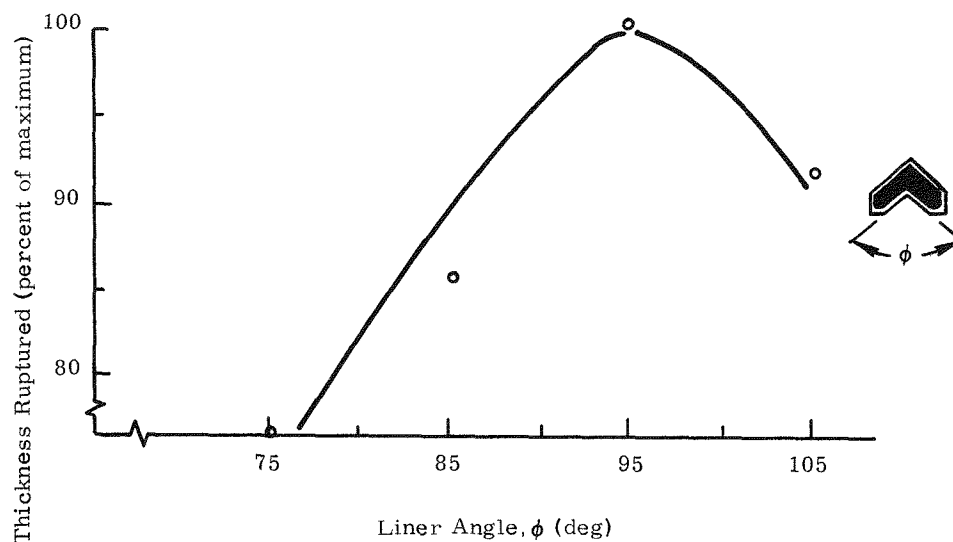


Figure VII-4. Optimum Standoff Distance

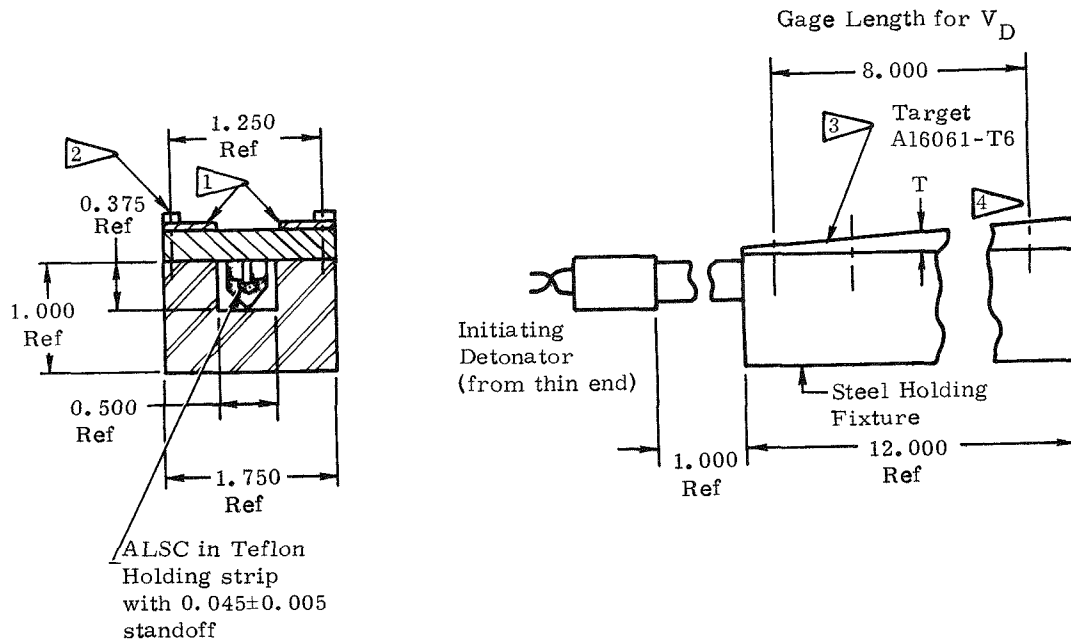
The optimum liner angle for 10-grain/foot ALSC was found to be 95 degrees. Data are shown in Figure VII-5.



Normalized for 10.0 grains/foot with a V_D of 6.95 mm/ μ sec,
a standoff of 0.045 inch and an aluminum target.

Figure VII-5. Optimum Liner Angle

Rupturing ability was determined by means of the tapered plate test fixture shown in Figure VII-6. Some test result differences, depending on whether the ALSC was initiated from the thin end or from the thick end of the plate, were noted. Generally, greater and more consistent rupturing was achieved from the thin-end initiations.



- 1 Mild steel holddown plate, 5/8 inch wide x 3/16 inch thick x 12 inch long.
- 2 Six round-head machine screws (steel) spaced at 2-inch intervals starting 1 inch from end. Torque to 35±5 inch-pounds.
- 3 Cross-rolled plates. Taper approximately 1/8 inch per foot.
- 4 Suggested midlength thickness of 0.120 inch for evaluating 10-grain/foot core load.

Reference: Sandia Specification SS 281496

Figure VII-6. Suggested Setup for Rupturing Ability and V_D Testing

It is important to note that rupturing ability is affected by ALSC confinement and the rigidity of the test plate. Therefore, data obtained in Figure VII-7 apply only to the test configuration used. It is suggested that these data be used only as a guide to determine the probability of success in a given application.

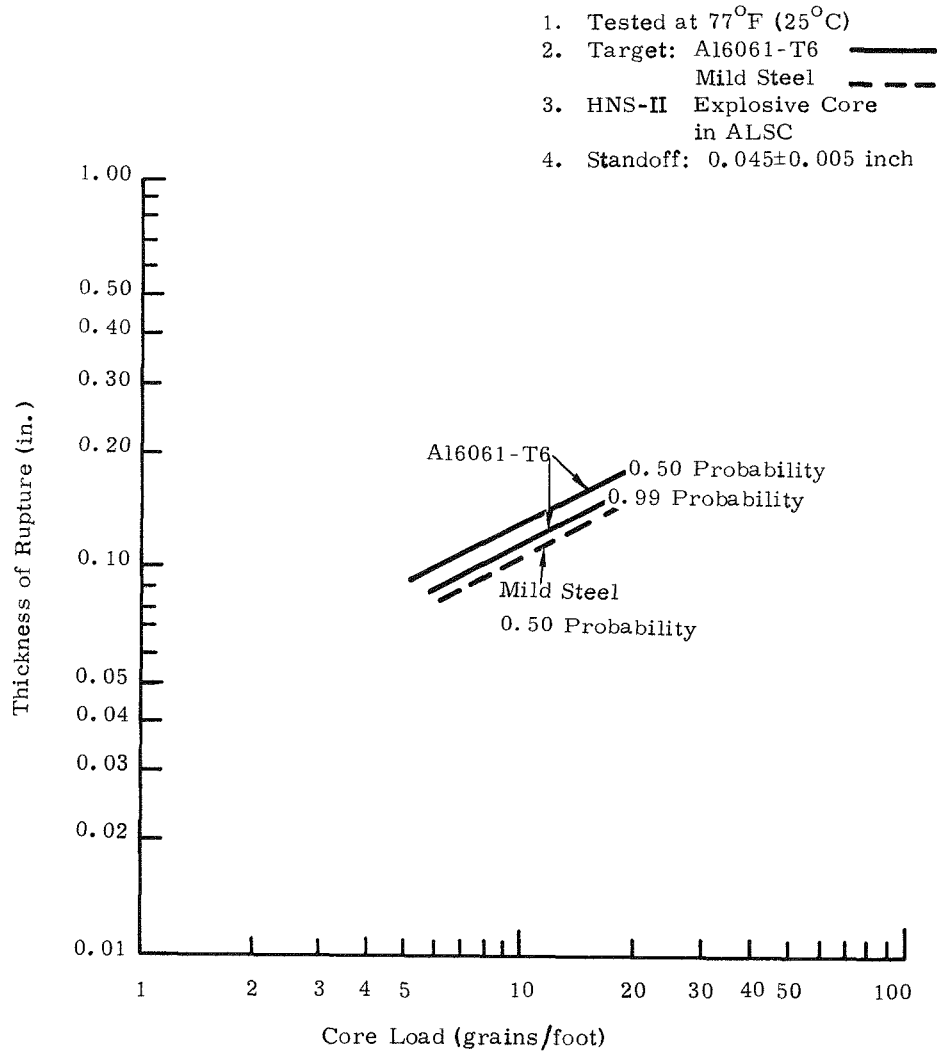


Figure VII-7. Effect of Core Load on Rupturing Ability of Aluminum 6061 and Mild Steel

Impulse Generated During Detonation

In most applications, the ALSC is required to perform a rupturing function in one direction without damaging its mounting structure in the opposite direction.

Accordingly, a test specimen was devised to measure the impulse generated as a function of explosive loading distribution (weight of explosive uniformly distributed over unit area). Impulse was determined by measuring the velocity of a flying plate whose weight was accurately known. The data apply to the specific configuration which included a relatively rigid back-up mass and good confinement. Figure VII-8 summarizes these results. Note that for values less than 0.02 gram/cm^2 , impulse was directly proportional to loading distribution. Edge effects and air resistance probably account for the nonlinearity of higher loading levels and are more pronounced for smaller test specimens.

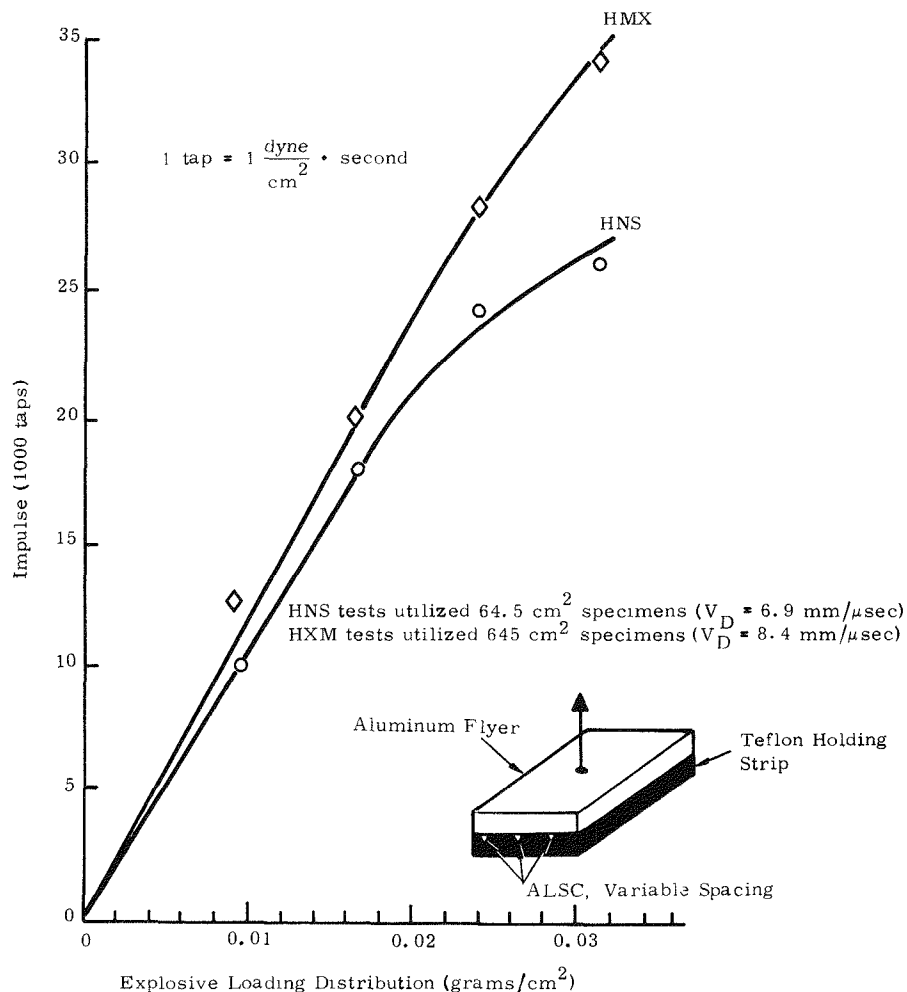


Figure VII-8. Effect of Loading Distribution on Impulse

Application Principles

The following relationships were established empirically during the experimentation previously described.

- (1) Effect of core load on the ability of ALSC to rupture aluminum

$$\frac{T_1}{T_2} = \left(\frac{W_1}{W_2} \right)^{0.58} .$$

- (2) Effect of target material on rupturing ability of ALSC

$$\frac{T_1}{T_2} = \left(\frac{\rho_2}{\rho_1} \right)^X \quad \text{where } X = 0.2 \text{ to } 0.7, \text{ depending on the hardness and the strength of target material.}$$

- (3) Effect of detonation velocity on rupturing ability of ALSC

$$\frac{T_1}{T_2} = \left(\frac{V_1}{V_2} \right)^X \quad X = 2.73 \text{ when detonation velocity changes as a result of thermal decomposition.}$$

X = 3 when detonation velocity changes as a result of density changes.

- (4) Impulse

$$\frac{I_1}{I_2} = \frac{W_1}{W_2} \quad \text{over the range of 0 to 0.02 gram of explosive/cm}^2 \text{ of surface area.}$$

T_1, T_2 = thickness of target material ruptured on 50 percent probability basis

W_1, W_2 = core load of ALSC used

ρ_1, ρ_2 = density of the target metal

V_1, V_2 = detonation velocity of HNS in ALSC

I_1, I_2 = impulse

SECTION VIII - ENVIRONMENTAL CAPABILITIES

Thermal Stability

Some of the thermal properties of HNS were included in Section II. However, in component applications, these criteria often fail to establish "use" limits. Thermal stability is more succinctly illustrated by the performance parameters discussed below. In deriving these data, 13-inch lengths of 10-grain/foot ALSC were subjected to a thermal aging treatment which consists of various time-temperature histories.

Detonation Velocity

Changes in detonation velocity at 75°F were noted as a function of time at elevated temperatures on specimens containing HNS, HNAB, HMX, and PETN. The data (Figure VIII-I) indicate that the explosives decomposed in a manner expected from isothermal decomposition.⁸ Data were plotted to indicate the combination of time and temperature which produced a 1 percent decrease in detonation velocity for each of the explosives; additional data for 5 and 10 percent decreases are shown for HNS; however, in practice, one would hesitate to allow this much decomposition.

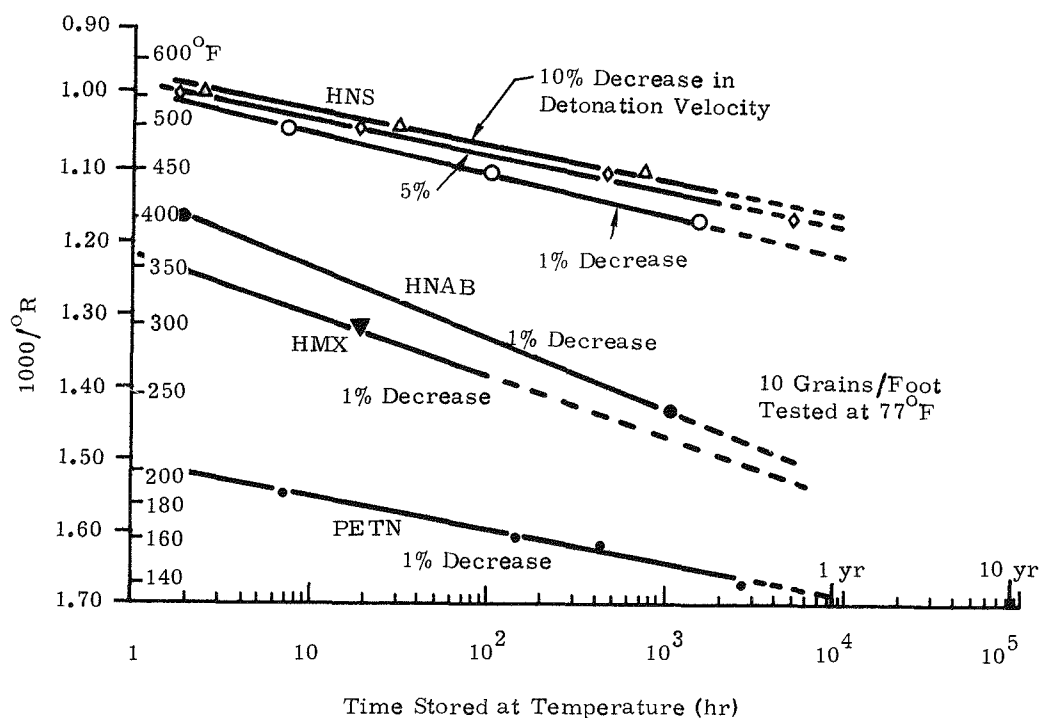


Figure VIII-1. Effect of Thermal Aging on Decrease in V_D of Various Explosive Materials

Rupturing Ability

The effect of thermal aging on rupturing ability was also noted for HNS in the experiment described above. A reduction in rupturing ability was noted, along with the decrease in detonation velocity. Average values are plotted in Figure VIII-2. The slope of the line indicated that rupturing ability was proportional to $V_D^{2.73}$ when detonation velocity was changed by decomposition. A small reduction in detonation velocity, V_D , produced a large reduction in rupturing ability.

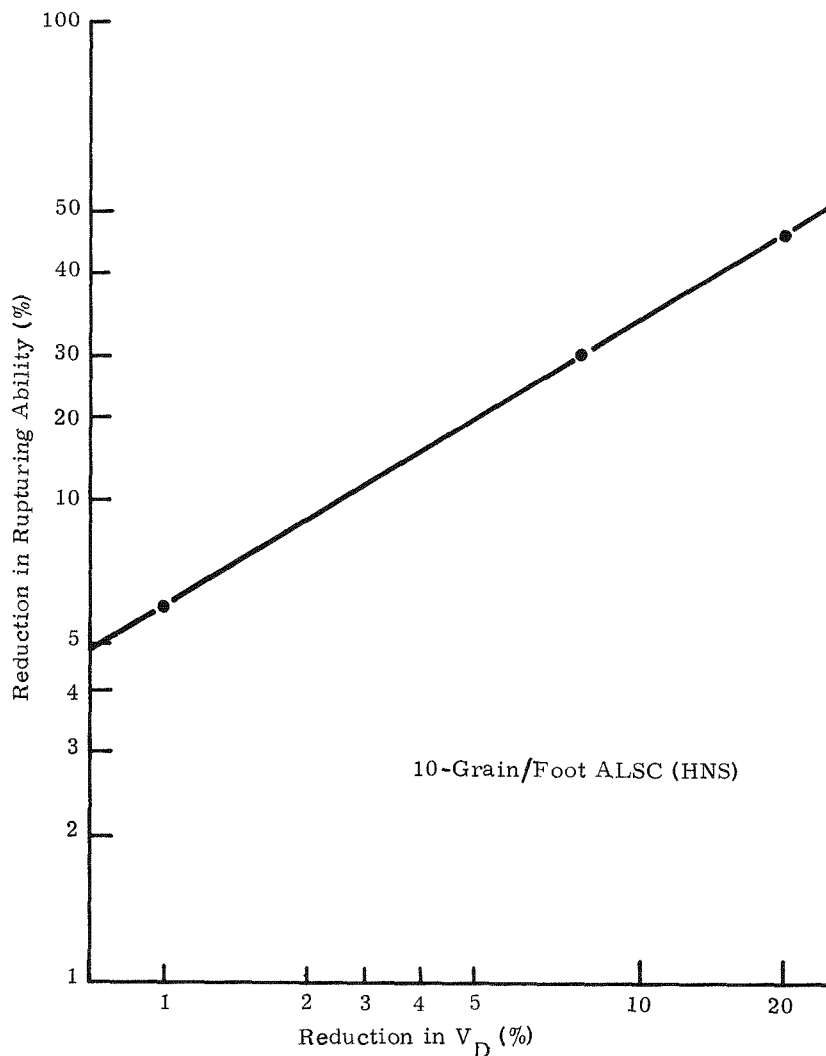


Figure VIII-2. Reduction in Rupturing Ability as a Function of Reduction in V_D Produced by Thermal Aging

Discoloration

The effect of thermal aging upon the color of the HNS was also noted. The photos of Figure VIII-3 illustrate the decomposition of HNS as a function of time at 500°F.

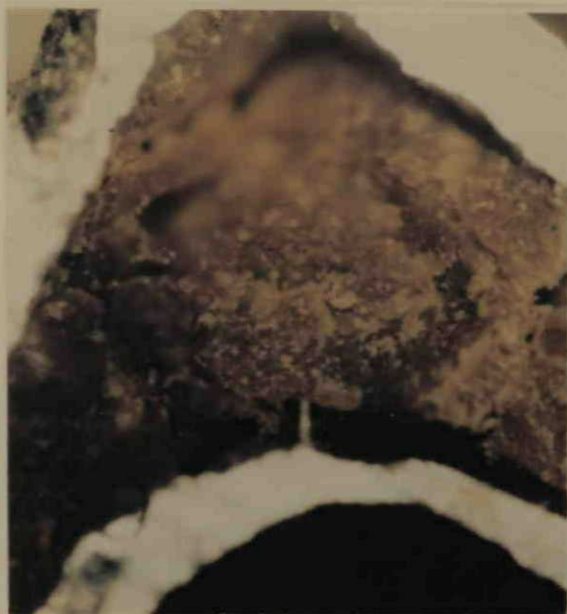
The sample which experienced 9 hours of exposure showed a 1 percent decrease in V_D , the 20-hour sample showed a 5 percent decrease, and the 33-hour sample showed a 10 percent decrease. Discoloration was not a precisely repeatable phenomenon.



Control



9 Hours at 500°F



20 Hours at 500°F



33 Hours at 500°F

End View of 10 gr/ft ALSC (HNS) (at 75X)

Figure VIII-3. Discoloration of HNS as a Result of Thermal Aging

Shock Initiation

Changes in initiation sensitivity at 75°F as a function of time stored at 500°F were observed. Data are shown in Figure VIII-4, along with detonation velocity changes. There was a significant increase in input pressure required for initiation, as well as a decrease in detonation velocity as time at temperature was increased. However, their rates of change were different.

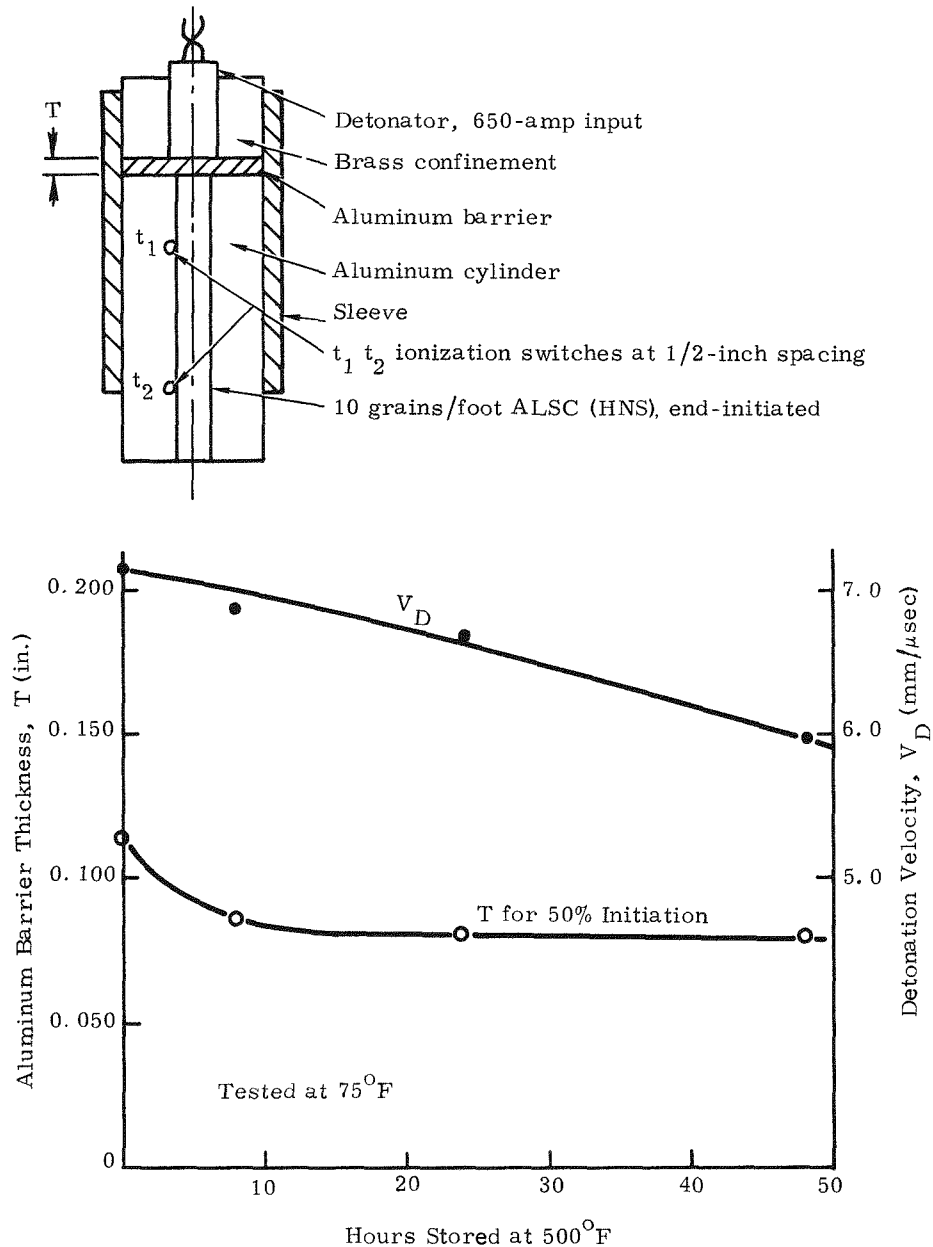


Figure VIII-4. Effect of Thermal Aging on Detonation Velocity and Barrier Thickness for 50 Percent Probability of Initiation of HNS

Weight Loss

Five-inch-long samples of 10-grain/foot ALSC (HNS) were exposed to 500°F, and weight loss was noted as a percentage of explosive weight at increasing time intervals. Data⁹ are shown in Figure VIII-5.

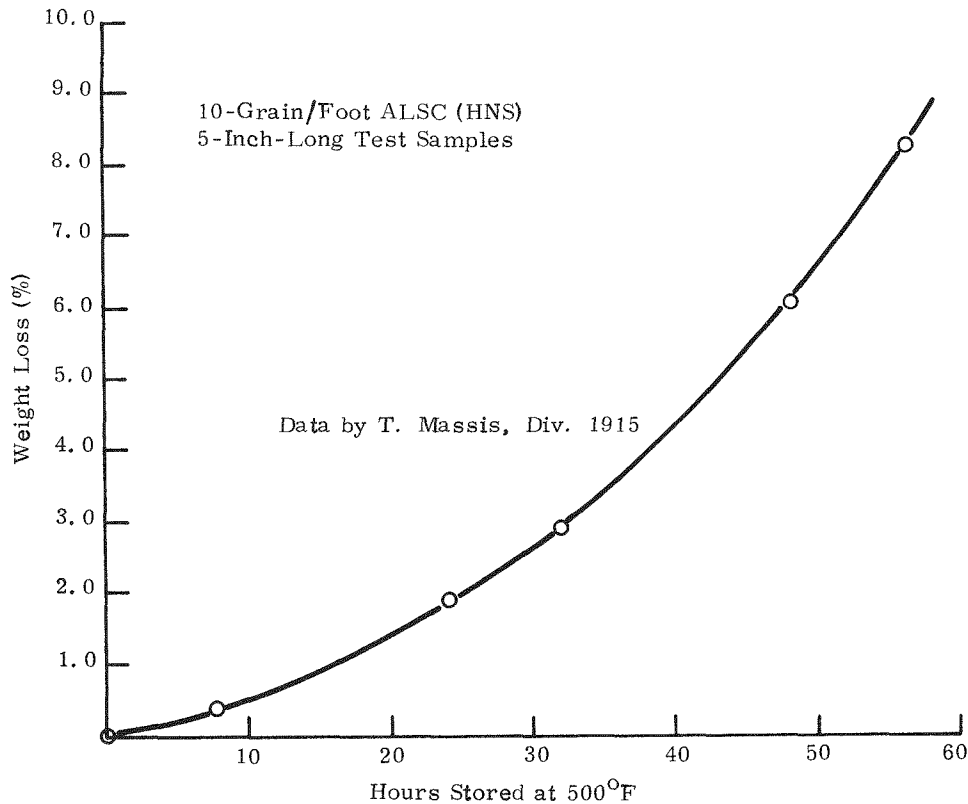


Figure VIII-5 Weight Loss vs Time at 500°F

Effect of Heating Rates

The reactions of HNS to a wide range of thermal flux rates, each of which provided a specific nonlinear temperature rise, are summarized in Figures VIII-6 and VIII-7

Tests were performed at Sandia's Radiant Heat Test Facility,¹⁰ with a focused quartz lamp as the heating source to provide thermal flux rates from 10 Btu/ft²-sec to 116 Btu/ft²-sec. The "reaction" temperature was observed for that point in time at which an audible "pop" was heard (but, in all cases, without high-order detonations); a discontinuity in the monitoring thermocouple output occurred concurrently. In the case for HMX, all explosive was consumed (several inches on each side of the exposed 1-inch length), but the aluminum sheathing remained; in the case for HNS, only that explosive directly exposed was consumed (the remaining lengths could be subsequently detonated). The reaction temperatures agree with those which might be expected in accordance with DTA data; HMX shows an exotherm at about 500°F and melts at 545°F; HNS melts at 608°F at a temperature below the exotherm at 660°F.

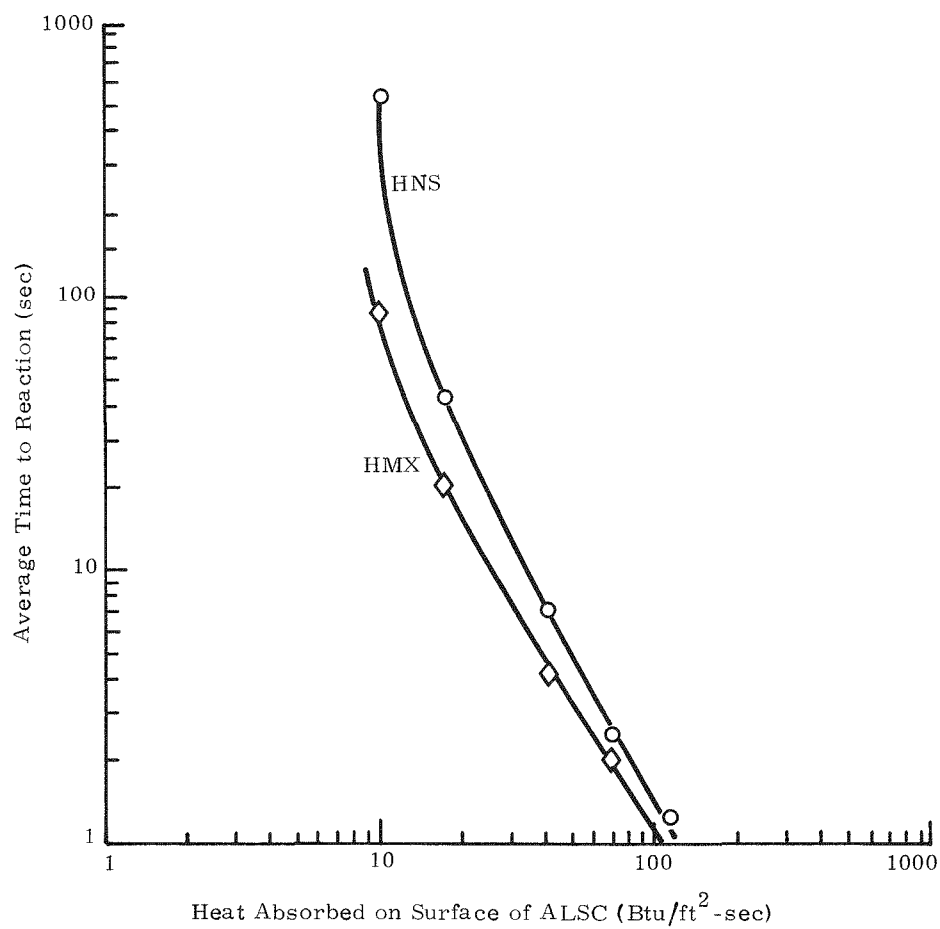


Figure VIII-6. Heat Absorbed on Surface of ALSC vs Time to Reaction

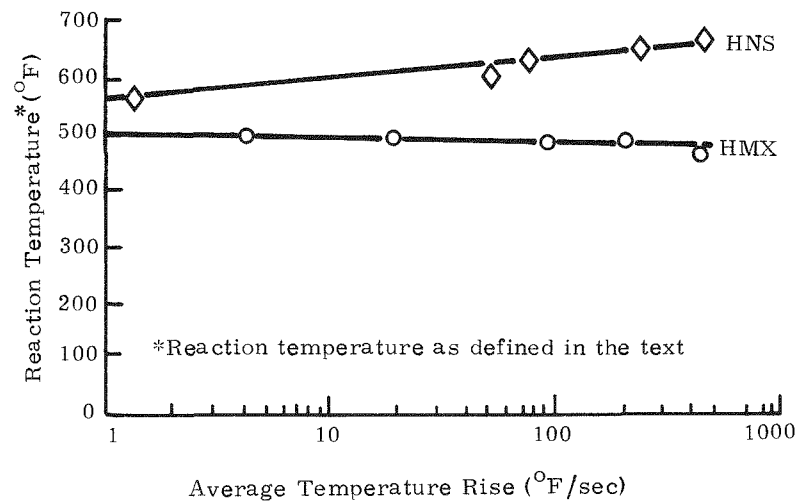


Figure VIII-7. Effect of Heating Rate on Reaction Temperature

Function at High Temperature

For those applications where function at elevated temperature is of concern, the data¹¹ of Table VIII-I apply. For the preconditioning and test temperature indicated, a 3 percent decrease in detonation velocity was noted. The instrumentation resolution was not adequate to distinguish any significant differences between the 350° and 500°F test data.

TABLE VIII-I

Effect of Temperature on Detonation Velocity (10-grain/foot ALSC (HNS))

<u>Precondition</u>	<u>Test (°F)</u>	<u>Measured Detonation Velocity (mm/ sec)</u>
None	77(25°C)	7.1
None	350(177°C)	---
None	500(260°C)	---
350°F, 10 Minutes	350(177°C)	6.8
350°F, 100 Minutes	350	6.9
350°F, 1000 Minutes	350	6.9
500°F, 10 Minutes	500(260°C)	6.9
500°F, 100 Minutes	500	6.9
500°F, 1000 Minutes	500	6.9

Radiation

The effects of nuclear reactor radiation on HNS, HNAB, PETN, and HMX were studied in detail by Avrami and Voreck.¹² This evaluation, during the period 1962-1968, included primary explosives, booster explosives, main-charge explosives, igniters, and propellants. Radiation effects on the following parameters were evaluated: weight loss, vacuum stability, gas release, explosion temperature, DTA, TGA, detonation velocity, melting point, and impact sensitivity.

Figure VIII-8 indicates the relative response of the four explosives with one prescribed value of weight loss as the criterion. Additional radiation data¹³ have been obtained.

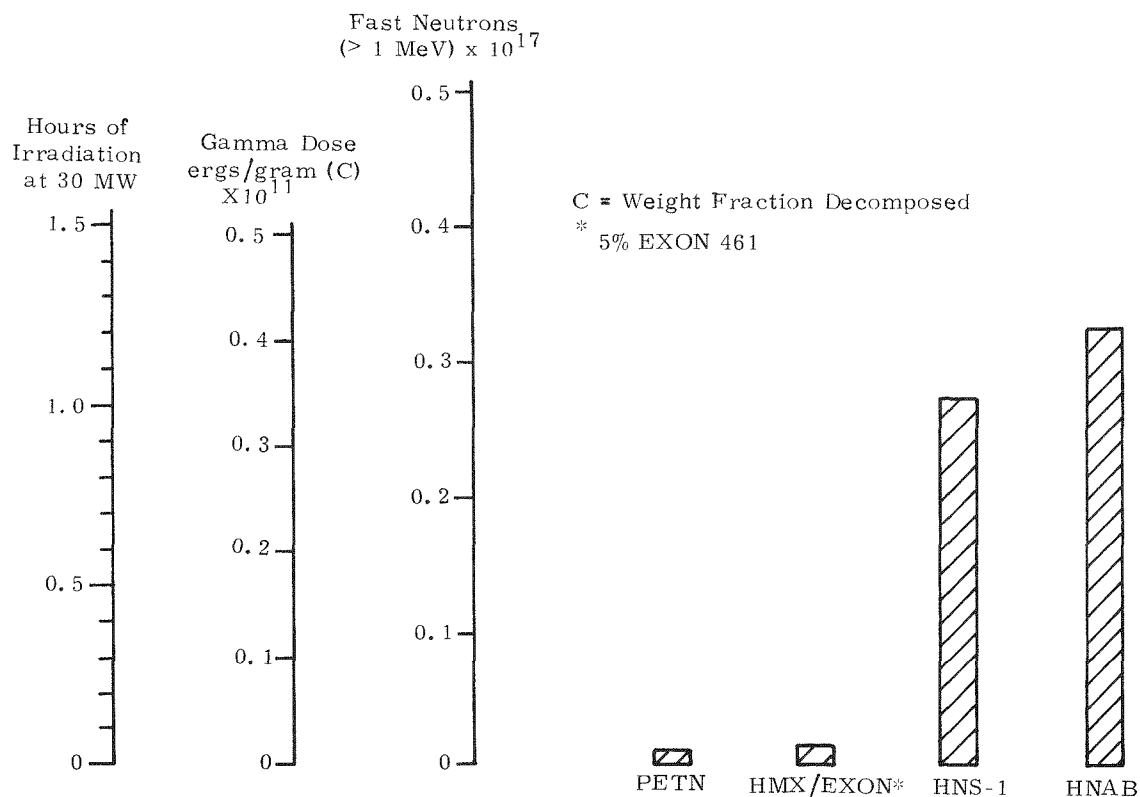


Figure VIII-8. Reactor Radiation Required to Produce a 1 Percent Weight Loss

Effect of Moisture

Samples of 10-grain/foot ALSC (HNS), each 2 inches long and without protective end caps, were exposed to 100 percent relative humidity for 528 hours at 75°F. Initiation sensitivity tests (axial mode) were subsequently performed with EX-12B detonators.

	Aluminum Barrier Thickness for 50 Percent Initiation (in.)		Detonation Velocity (mm/ μ sec)	
	Average	Range	Average	Range
Control Units	0.125	0.005	6.84	0.01*
Exposed Units	0.125	0.030	6.85	0.25

The moisture produced little change in the average response, but greater variability was experienced.

* Two-point data

High Altitude (low pressure)

The low vapor pressure exhibited by HNS makes it an ideal candidate for high-altitude and space applications.¹⁹

Evaluations at Sandia are summarized in Table VIII-II. Effects of low pressure, for brief or long periods, on rupturing ability are indicated. One measurement of impulse is also indicated.

TABLE VIII-II

Summary of High-Altitude Tests (10-grain/foot ALSC (HNS))

Laboratory Tests				
Test	Description	Environment	Results	
			Average Detonation Velocity (mm/μsec)	Average Rupturing Ability (in.)
6 ea	Controls	Normal	6.94	0.128
6 ea	Test Specimens	100,000-ft altitude, 120°F	6.91	0.144
Laboratory Subsystem Tests				
1 ea	Cylindrical Panel Axial Rupture	195,000 ft (at 0.2 mm hg)	Satisfactory rupture. Measured impulse was 17,000 taps at 0.02 gram HE/cm ² compared to approximately 20,000 taps control data.	
2 ea	SDT/Adapter/ALSC	225,000 ft (at 0.05 mm hg after 1 week of exposure)	Satisfactory function.	
Field Tests				
2 ea	Nike-Nike Rocket With Payload	10,000 ft	Satisfactory rupture by a total of 24 each of 5-foot-long pieces.	
1 ea	HAT Vehicle With Payload	70,000 ft	Satisfactory rupture by a total of 4 each of 12-foot-long pieces.	

SECTION IX - TYPICAL APPLICATIONS OF HNS

Aluminum-Sheathed Linear Shaped Charge

Uses of ALSC include stage separation and emergency escape in the aerospace industry and a variety of functions in ordnance hardware. It is used in applications where its limited flexing is permissible and where high temperature, low weight, and radiation resistance materials are desirable. It is ideally suited to space applications where its low vapor pressure is advantageous. It provides a new level of safety in that its explosive insensitivity is greater than that for PETN.

Figure IX-1 shows 10-grain/foot ALSC supported in a teflon holding strip. ALSC may be produced from Sandia specification SS-281496. Approximately 3500 feet of ALSC have been produced since August 1968. Several failures to initiate were experienced prior to the establishment of an adequate input level.

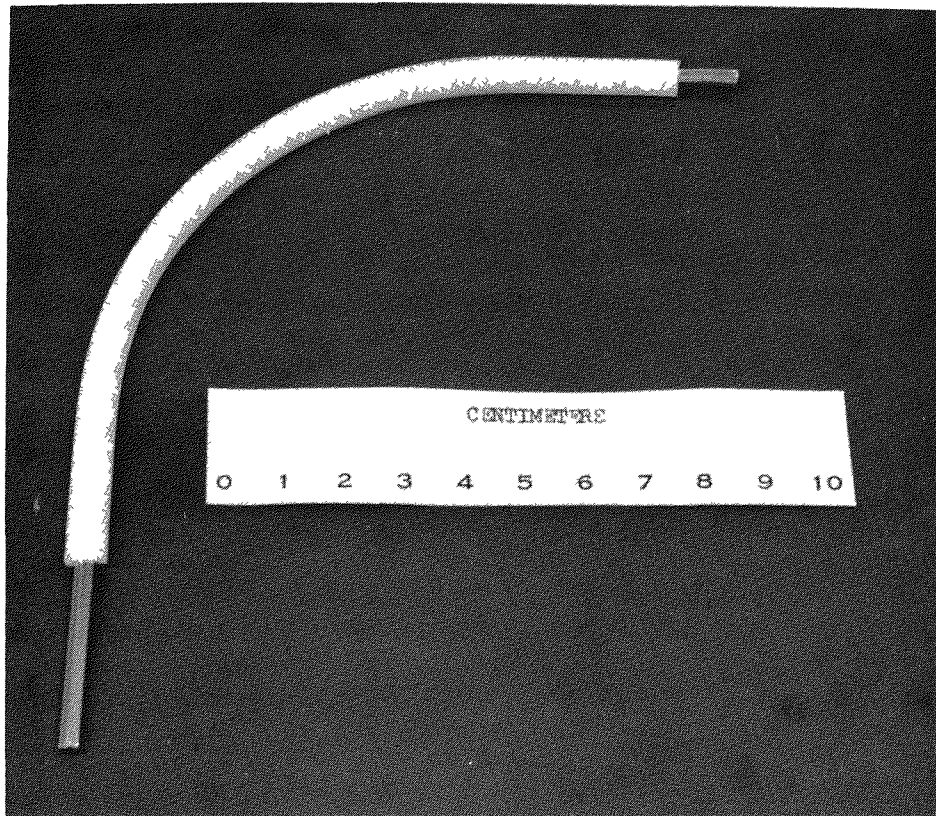


Figure IX-1. ALSC in Teflon Holding Strip
(10 grains/foot)

Shielded Detonating Train

The predecessor of SDT was developed for use in the F-111 ejectable crew module¹⁵ to transfer the explosive shock near personnel to the many explosive devices used. Explosive functions include operating emergency oxygen valves, actuating cable cutters, igniting rocket motors, activating shaped charges, and deploying parachutes. SDT consists of a length of 2-1/2-grain/foot MDF inside teflon tubing, which, in turn, is inside high-strength stainless steel tubing of 3/16-inch outside diameter. Each end is fitted with 105 milligrams of HNS inside a stainless cup. These ends serve as donors or acceptors and are the only portions which fragment, inasmuch as the MDF is fully contained within the tubing.

Figure IX-2 is a cross-sectional view of SDT (also referred to as SMDC in the F-111 application). SDT differs from SMDC in that it employs HNS in the MDF and employs an aluminum sheathing instead of silver.

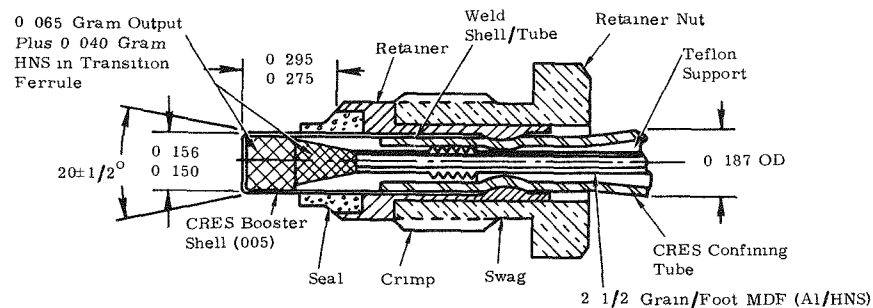


Figure IX-2. Cross Section, SDT Tip

Figure IX-3 shows SDT being used in a typical distribution train. The specification for procurement of SDT is contained in Drawing SS 293079. Approximately 150 pieces have been procured by Sandia and successfully test fired since July 1969.

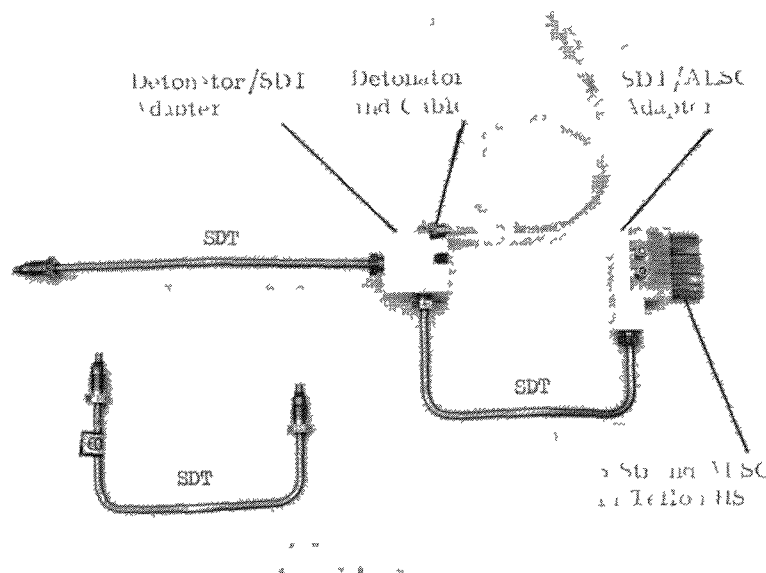


Figure IX-3. SDT Distribution Train

Mild Detonating Fuze

MDF, in the circular cross section, or RMDF, in the rectangular cross section, is used in many applications where shock transfer is required. Both forms have the capability to provide precision timing delays between fixed lengths. RMDF offers an excellent means to transfer explosive shocks across large air gaps (to several inches) and, recently, has been used* in explosive welding.¹⁸ Environmental capabilities are equivalent to those enumerated for ALSC.

MDF may be fabricated by swaging and/or drawing to final size. The outside diameter of 1 grain/foot is approximately 0.032 inch and of 10 grains/foot is 0.110 inch.

Figure IX-4 shows aluminum-sheathed MDF in typical sizes. The Sandia specification for procurement is SS 293081. Seven hundred feet of MDF and 400 feet of RMDF have been procured by Sandia since November 1969.

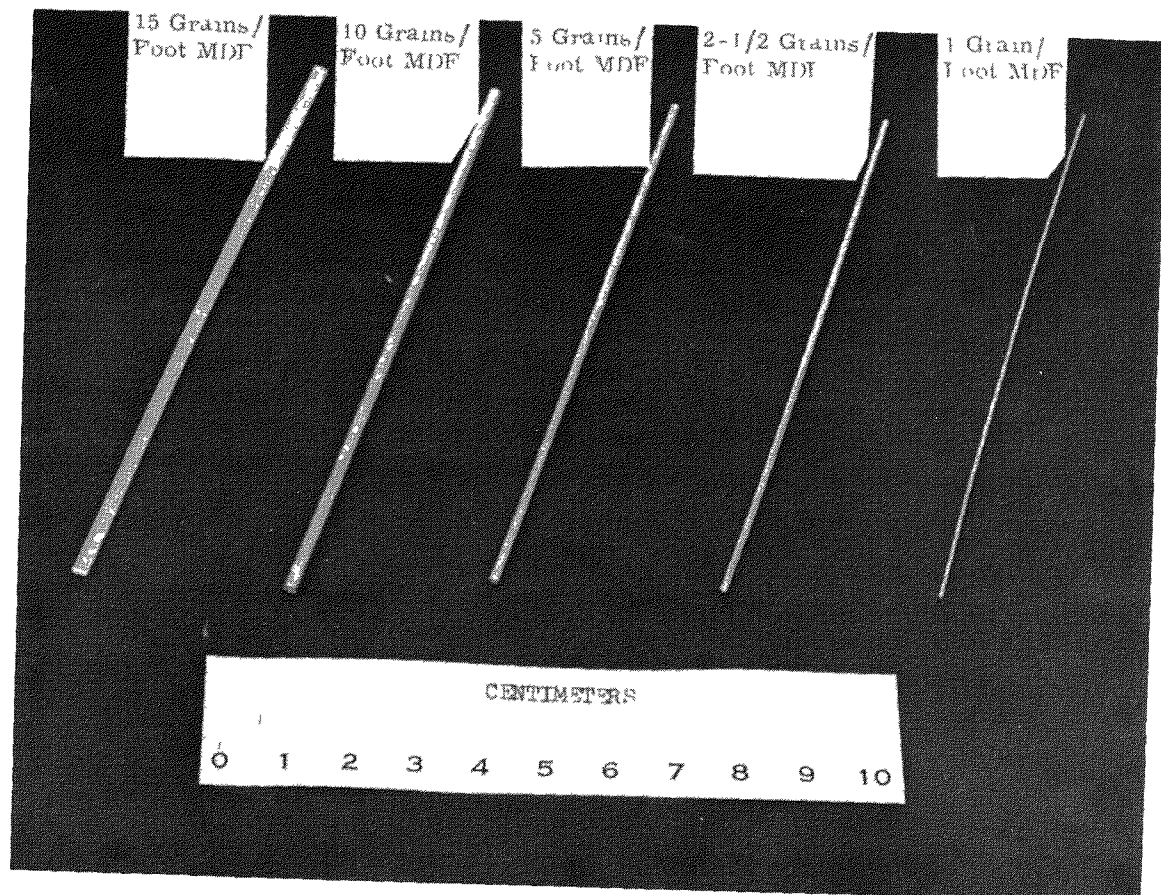


Figure IX-4. MDF

* Not with HNS, although this should not be technically unsound.

End Fittings

End fittings are used to seal or cap lengths of ALSC and MDF. They are extruded to fit the chevron or circular cross sections and are loaded with HNS-1 explosive, with a column height greater than the column diameter and a powder density of 1.55 ± 0.05 grams/cm³.

Compatible adhesives may be used to secure the end fittings in place. Aluminum extrusions of 0.010 ± 0.001 -inch wall thickness are used. Sandia specifications are in process.

Typical fittings are shown in Figure IX-5. Five hundred ALSC fittings and 300 MDF fittings have been procured since September 1970. Intentional failures were generated when (1) an incompatible adhesive was used, (2) the wall thickness exceeded specification, and (3) an air gap was provided in the powder train. Defects (2) and (3) were identified by radiographic inspections, and compatible adhesives have been identified.

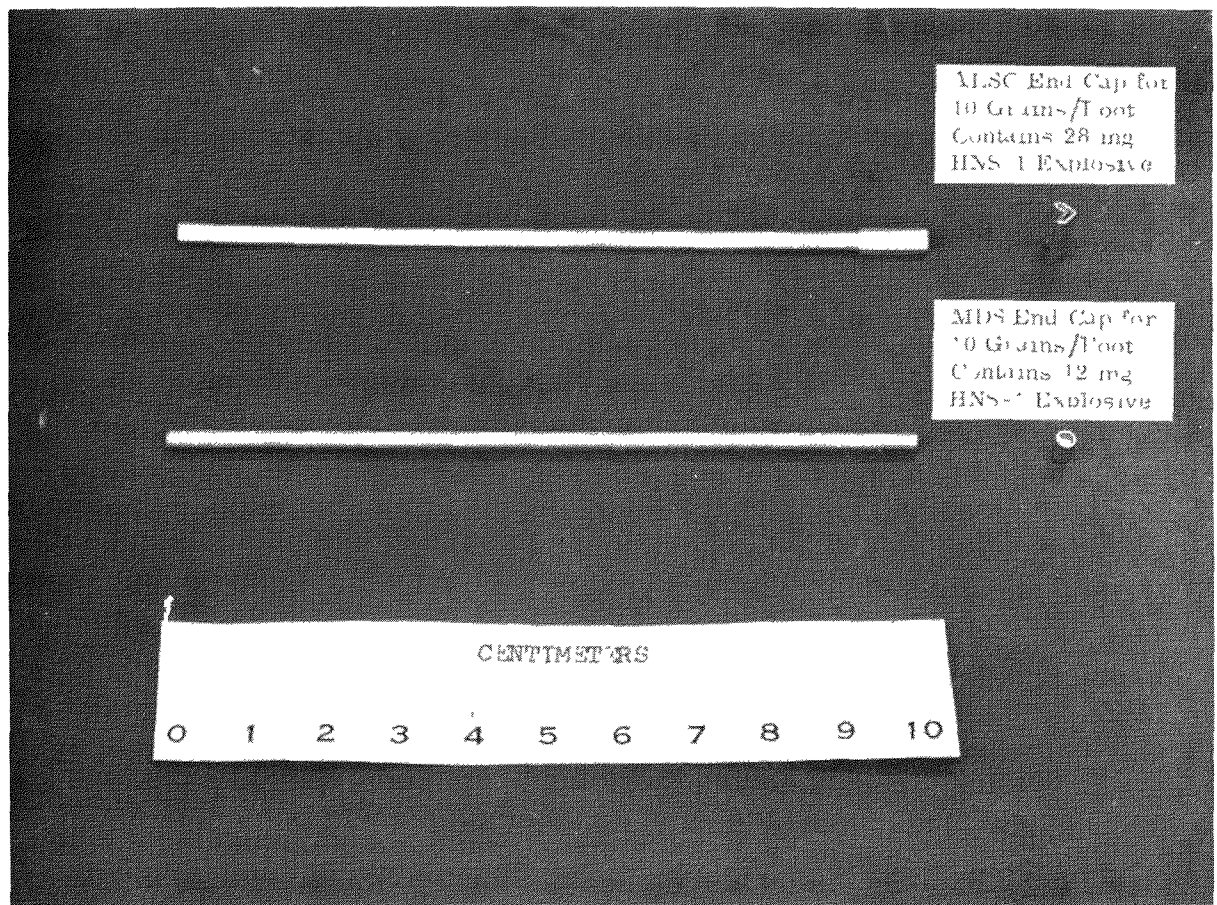


Figure IX-5. End Fittings

SECTION X - REFERENCES

1. E. E. Kilmer, "Heat-Resistant Explosives for Space Applications," Journal of Spacecraft, Volume 5, No. 10, October 1968.
2. E. E. Kilmer, "The Application of Heat Resistant Explosives to Advanced Weapons and Space Systems," Proceedings of the Sixth Symposium on Electroexplosive Devices, July 8-10, 1969, Confidential Paper 5-2.
3. Kathryn G. Shipp, "Properties of Selected Thermally Stable Explosives (U)," Confidential Report NOLTR 70-95, dated May 21, 1970.
4. R. H. Stresau, Sandia Contractor Report, SC-CR-70-6076, dated May 1970, performed on Sandia Contract 58-6740. Data were also extracted from final reports on Contracts 58-6975, 25-9070, and 25-9574, with Stresau Laboratory, Spooner, Wisconsin.
5. Unclassified Memorandum, T. M. Massis to A. C. Schwarz, dated December 24, 1970, Subject: "HNS-MDF Core Data (U)."
6. R. J. Buxton and T. M. Massis Compatibility of Explosives With Structural Materials of Interest (U), "SC-M-70-355, August 1970.
7. Report No. 1, dated May 26, 1970, and Report No. 2, dated June 15, 1970, on Sandia Contract 58-8591, with Stanford Research Institute, Menlo Park, California, R. J. Buxton, Sandia Corporation Consultant.
8. M. A. Cook, The Science of High Explosives (P 174), Reinhold Publishing Corporation.
9. Unclassified Memorandum, T. M. Massis to A. C. Schwarz, dated March 10, 1971, Subject: "500°F HNS Weight Loss."
10. P. H. Adams et al, The Sandia Corporation Radiant Heat Facility, SC-RR-67-438, dated August 1967.
11. G. W. Neff, Final Report on Sandia Contract 93-1624, performed by Mason & Hanger (Pantex Plant).
12. Louis Avrami and Wallace Voreck, A Determination of Reactor-Radiation-Resistant Explosives, Propellants, and Related Materials (U), Picatinny CRD Report 3782, dated November 1969.
13. SRD Report, SC-DR-69-451 (Part 1), dated July 1969, Sandia Corporation RS3410/1475.
14. L. D. Pitts, "Designing Electro-Explosive Devices for Electrostatic Insensitivity," Paper 2-7, Proceedings of the 5th EED Symposium, June 13-14, 1967.
15. R. L. Atkins, The F-111 Crew Module, General Dynamics Report, FZM-12-4094B, dated February 1, 1968.
16. C. H. Johansson and P. A. Peters, Detonics of High Explosives, Academic Press, New York.
17. R. H. Stresau, Report RSLR 70-11-2, dated December 23, 1970 on Sandia Corporation Contract 25-9564.
18. Laurence J. Bement, "Welding of Aluminum With Linear Ribbon Explosives," Paper IV-2, Proceedings of the 7th Symposium on Explosives and Pyrotechnics, Sept. 8-9, 1971. Lead-sheathed, RDX-core ribbon was used.
19. Laurence J. Bement, "Application of Temperature-Resistant Explosives to NASA Missions," presented at Symposium on Thermally Stable Explosives at the Naval Ordnance Laboratory, June 23-25, 1970.

DISTRIBUTION:

U. S. Naval Ordnance Laboratory
White Oak, Silver Spring, MD 20910
Attn: E. E. Kilmer,
Explosions Research Dept.
Kathryn G. Shipp,
Chemistry Research Dept.

Ensign Bickford Co.
660 Hopmeadow Street
Simsbury, CT 06070
Attn: Phil Murphy
Brian Boggs
D. F. Elliot

G. B. Huber
Explosive Technology
P. O. Box KK
Fairfield, CA 94533

Lawrence Livermore Laboratory
P. O. Box 808
Livermore, CA 94550
Attn: John Stroud
R. C. Meyers

W. B. Hopson
Jet Research Center, Inc.
P. O. Box 246
Arlington, TX 76010

R. Stresau
R. Stresau Laboratory
Spooner, WI 54801

Howard Anderson
Teledyne-McCormick Selph
P. O. Box 6
Hollister, CA 95023

McDonnell Douglas Astronautics Company
Huntington Beach, CA 92647
Attn: S. A. Moses

McDonnell Douglas Corp.
P. O. Box 516
St. Louis, MO 63166
Attn: V. W. Drexelius
M. L. Shimmel

Picatinny Arsenal
Dover, NJ 07801
Attn: Don Seeger
W. Voreck

Gunther Cohn
The Franklin Institute Research Labs
Philadelphia, PA 19103

Laurence J. Bement
NASA - Langley Research Center
Langley Station
Hampton, VA 23365

Clarence Simpson
Unidynamics/Phoenix, Inc.
P. O. Box 2990
Phoenix, AZ 85036

George E. Sheridan
Reynolds Industries, Inc.
P. O. Box P850
Marina Del Rey, CA 90291

Ted Blechar
Lockheed Missiles and Space Co.
P. O. Box 504
Sunnyvale, CA 94088

Los Alamos Scientific Laboratory
P. O. Box 1663
Los Alamos, NM 87544
Attn: Al Popolato, GMX-3
R. H. Naffziger, GMX-3
R. L. Spaulding, GMX-7

T. J. Graves
National Aeronautics and Space Administration
Manned Spacecraft Center
Houston, TX 77058

L. LoFiego
Bermite Division, Tasker Industries
22116 West Soledad Canyon Road
Saugus, CA 91350

L. C. Yang
Jet Propulsion Laboratory
California Institute of Technology
4800 Oak Grove Drive
Pasadena, CA 91103

Carl King
Mound Laboratory
Monsanto Research Corporation
Miamisburg, OH 45342

I. B. Akst
Mason & Hanger, Silas Mason Co.
P. O. Box 647
Amarillo, TX 79105

Reginald F. Page
Bell Telephone Laboratories
Whippany, NJ 07981

K. D. Bowers, 10
W. C. Myre, 1210
R. L. Peurifoy, 1220
L. D. Smith, 1300
C. B. McCampbell, 1310
J. J. Marron, 1314
H. M. Barnett, 1315
W. A. Gardner, 1500
D. M. Olson, 1510

DISTRIBUTION (Cont.)

C. C. Burks, 1511
C. H. Mauney, 1530
T. B. Lane, 1540
W. E. Alzheimer, 1551
B. E. Arthur, 1640
H. E. Walker, 1641
W. L. Stevens, 1650
C. Winter, 1710
R. G. Clem, 1730
A. A. Lieber, 1750
J. C. King, 1900
D. H. Anderson, 1910
R. D. Wehrle, 1912
B. H. Van Domelen, 1913
J. P. Weber, 1914
A. C. Schwarz, 1914 (5)
P. E. Matson, 1914
E. A. Kjeldgaard, 1915
R. J. Buxton, 1915
T. M. Massis, 1915
J. E. Gover, 1935
J. E. Kennedy, 5131
R. C. Maydew, 5620

L. J. Heilman, 7400
R. H. Schultz, 7420
W. C. Kraft, 7430
Attn: J. T. Hilman, 7434
R. W. Devore, 7620
J. B. Wright, 8131
O. H. Schreiber, 8139
D. E. Gregson, 8150
G. L. Scholer, 8153
R. A. Baroody, 8160
G. E. Brandvold, 8170
R. H. Meinken, 8310
G. W. Anderson, 8330
J. L. Wirth, 8340
C. F. Bild, 9100
M. L. Kramm, 9210
J. H. Davis, 9224
E. L. Harley, 9225
R. Hepplewhite, 9240
M. Cowan, 9320
D. S. Dreesen, 9342
L. S. Ostrander, 8232
R. S. Gillespie, 3151 (3) (for public release)
W. K. Cox, 3141-1 (16)

g/c/e